DISCLAIMER:

This document does not meet the
current format guidelines of
the Graduate School at
The University of Texas at Austin.

It has been published for
informational use only.

The Thesis Committee for Caroline Croft Hackett
certifies that this is the approved version of the following thesis:

Storage dynamics of the upper Nueces River alluvial aquifer: Implications for recharge to the Edwards Aquifer, Texas

APPROVED BY
SUPERVISING COMMITTEE:

Supervisor:

Daniella M. Rempe, Supervisor

Marcus O. Gary, Co-Supervisor

Storage dynamics of the upper Nueces River alluvial aquifer: Implications for recharge to the Edwards Aquifer, Texas

by

Caroline Croft Hackett

Thesis
Presented to the Faculty of the Graduate School of
The University of Texas at Austin
in Partial Fulfillment
of the Requirements
for the Degree of

Master of Geological Science

The University of Texas at Austin
2019

Abstract

Storage dynamics of the upper Nueces River alluvial aquifer: Implications for recharge to the Edwards Aquifer, Texas

Caroline Croft Hackett, M.S. Geo. Sci.
The University of Texas at Austin, 2019

Supervisor: Daniella M. Rempe

The karstic Edwards Aquifer is a crucial water resource in south-central Texas, serving as the primary water source for over two million people in the greater San Antonio area. The Nueces River basin is the largest contributor of recharge to the Edwards Aquifer, and recharge has traditionally been measured as the difference between river discharge at the upstream and downstream ends of the Edwards Group outcrop (Edwards Aquifer Recharge Zone, EARZ). This study investigated the extent to which groundwater in alluvial terraces and younger, near-channel alluvium deposits impact the timing and magnitude of recharge from the Nueces basin. Estimates of alluvial storage derived from geologic maps and sparse groundwater data suggest that over 21,000 acre-feet (25.9 x 10^6 m^3) of groundwater are stored in the upper Nueces River alluvial aquifer, with an estimated maximum capacity of over 75,000 acre-ft (92.5 x 10^6 m^3). However, the dynamics of alluvial bank storage and drainage from the alluvial aquifer and their impacts on downstream recharge are unknown. In this study, river water storage and transport in alluvium were investigated using differential gaging, dye tracer testing, baseflow recession analyses, and floodplain groundwater mass balances. Field investigations were made at a gaged, alluvium-lined

reach of the Nueces River where the river partially supplies a major tributary that maintained baseflow during the 2011 drought (whereas river flow ceased). Significant streamflow losses in the study area are largely the result of storage in high conductivity gravels adjacent to the channel, with some recharge to the alluvial aquifer and discrete recharge into bedrock. The baseflow contribution from the upper Nueces River alluvial aquifer contributes up to 100% of river flow during low flow conditions in the basin. The magnitude and shape of baseflow recession is dynamic between the growing and dormant seasons. These findings have implications for groundwater pumping from the upper Nueces River basin alluvial aquifer and the management of recharge to the Edwards Aquifer.

Table of Contents

List of Figures

List of Tables

1. Introduction and Background

Introduction

In central Texas, USA, the karstic Edwards Aquifer is located within the Edwards Plateau region, composed primarily of Cretaceous-age limestone (Clark, 2003). It is the primary drinking water source for more than two million people in the greater San Antonio, Texas, area and supplies industry and agriculture across the south-central part of the state (Sharp et al., 2019). The Edwards Aquifer is actually a set of aquifers that are variably connected across the extent of the system; the Edwards Aquifer System is divided by region into the Edwards-Trinity (Plateau) Aquifer, the Edwards (Balcones Fault Zone) Aquifer, and the Edwards (Washita Prairies) Aquifer (Sharp et al., 2019). Accurate calculations of total recharge are essential to the sustainable management of the Edwards Aquifer. Recharge in karst areas is divided into several components: allogenic recharge from precipitation falling on upstream drainage areas; autogenic recharge from precipitation over the recharge area; and leakage from other units or aquifers (Hauwert and Sharp, 2014). The majority of recharge to the Edwards Aquifer is estimated as discrete autogenic recharge from streambeds within the Edwards Aquifer Recharge Zone, where the Edwards Group limestone outcrops (Puente, 1978; Woodruff and Abbott, 1979; Hauwert, 2016). Diffuse autogenic recharge occurs outside of stream reaches and is often estimated as a fraction of annual precipitation. In a study of the Barton Springs segment of the Edwards Aquifer, Slade (2014) estimated only 26% of total recharge is from the area outside of stream channels, representing 9% of precipitation over the recharge area. Also in the Barton

Springs segment, Hauwert and Sharp (2014) used a water balance approach to calculate diffuse autogenic recharge in a small, internal drainage sinkhole basin to be 26% of rainfall. Recharge in the San Antonio segment of the Edwards (Balcones Fault Zone) Aquifer is monitored and reported by the U.S. Geological Survey (USGS) and the Edwards Aquifer Authority (EAA), a regulatory agency created by the State of Texas for the protection and management of the aquifer. The USGS calculates recharge to the Edwards Aquifer as the difference between stream discharge measurements upstream and downstream of the Recharge Zone for each river basin in the zone (Puente, 1978).

Several of the major river basins of the Edwards Plateau have mantled alluvial aquifers that could have a significant impact on the magnitude and timing of river discharge, and thus have an impact on discrete recharge to the Edwards Aquifer. Many studies exist that have evaluated interactions of surface water and groundwater in an alluvial floodplain, including studies of the impact of high hydraulic conductivity preferential flow paths (Miller et al., 2016). Heeren et al. (2014) demonstrated that alluvial floodplains can act as bank storage zones that can rapidly store then release flood discharge. However, few studies have evaluated the role of alluvium mantled over a karst floodplain. A few researchers have investigated the role of alluvium in buffering floods in a karst landscape. Keshavarzi et al. (2016) observed the transmission of river water through a karst-alluvial aquifer in Wellington, Australia, based on groundwater level changes in a cave system. Raeisi (2008) used groundwater measurements in an alluvial aquifer adjacent to a karst system to estimate inflows and outflows from the karst aquifer. Green (2008)

estimated discharge from the karstic Edwards Aquifer as underflow from the Leona River alluvial floodplain. Very few studies have examined the temporal effects of storage of river water in alluvium on recharge to a downstream karst aquifer.

This research examines surface water-groundwater interactions within the upper Nueces River basin. The Nueces River is the westernmost watershed of the Edwards Plateau. The upper basin is part of the Edwards-Trinity (Plateau) Aquifer, one of the three provinces of the Edwards Aquifer System (Sharp et al., 2019). The upper basin is also considered to be part of the Edwards Aquifer Contributing Zone, since streamflow originating in this area becomes recharge to the Edwards (Balcones Fault Zone) Aquifer where the Nueces River crosses into the Edwards Aquifer Recharge Zone. During the period of 2007 – 2016, the Nueces River basin contributed an average of 23% (151,500 af/yr or 187 x 10^6 m^3/yr) of total annual Edwards Aquifer recharge (669,400 af/yr or 826 x 10^6 m^3/yr), as calculated with the USGS method (EAA, 2017). This was the largest contribution among the nine major river basins that provide recharge to the Edwards Aquifer. Over the entire period of record from 1934 – 2016, the Nueces basin contributed an average of 18% (128,000 af/yr or 158 x 10^6 m^3/yr) of total annual recharge (706,500 af/yr or 871 x 10^6 m^3/yr), the second-most of all basins (EAA, 2017). Importantly, stream discharge gain-loss surveys within the Edwards Aquifer Contributing Zone of the upper Nueces basin reveal significant streamflow losses in this zone as well. I hypothesize that discharge losses in the upper Nueces basin are partitioned between storage in alluvium and recharge into karst features. The extent to which alluvial storage impacts the magnitude

and timing of Nueces River discharge is unknown. I hypothesize that discharge from the alluvial storage to the Nueces River could be significant year-round and is especially important during dry seasons and extended drought periods.

This study investigates the effects of river water storage in alluvium within the upper Nueces River basin on modifying or buffering recharge downstream in the Edwards Aquifer Recharge Zone. Using hydrograph analyses, I examine whether drainage from bank storage and from the alluvial aquifer extends the temporal opportunity for recharge due to the time lag of groundwater discharge to the river. Additionally, I put first order constraints on the possibility of drainage from the alluvial aquifer into the underlying Edwards-Trinity (Plateau) Aquifer via discrete karst recharge features. I investigate shallow groundwater flowpaths in the study area near Montell, TX, (Figure 1) where the Nueces River loses up to 68% of flow in wet basin conditions and 100% of flow during dry periods. Using fluorescent dye tracer testing, differential gaging, and groundwater mass balance calculations, I investigate the source of springflow on a major tributary that is used as a representative case study. The results from this study could impact decisions about groundwater extraction from the upper Nueces alluvial aquifer and can be used to determine whether Edwards Aquifer recharge calculations should account for Nueces River losses within the Edwards Aquifer Contributing Zone.

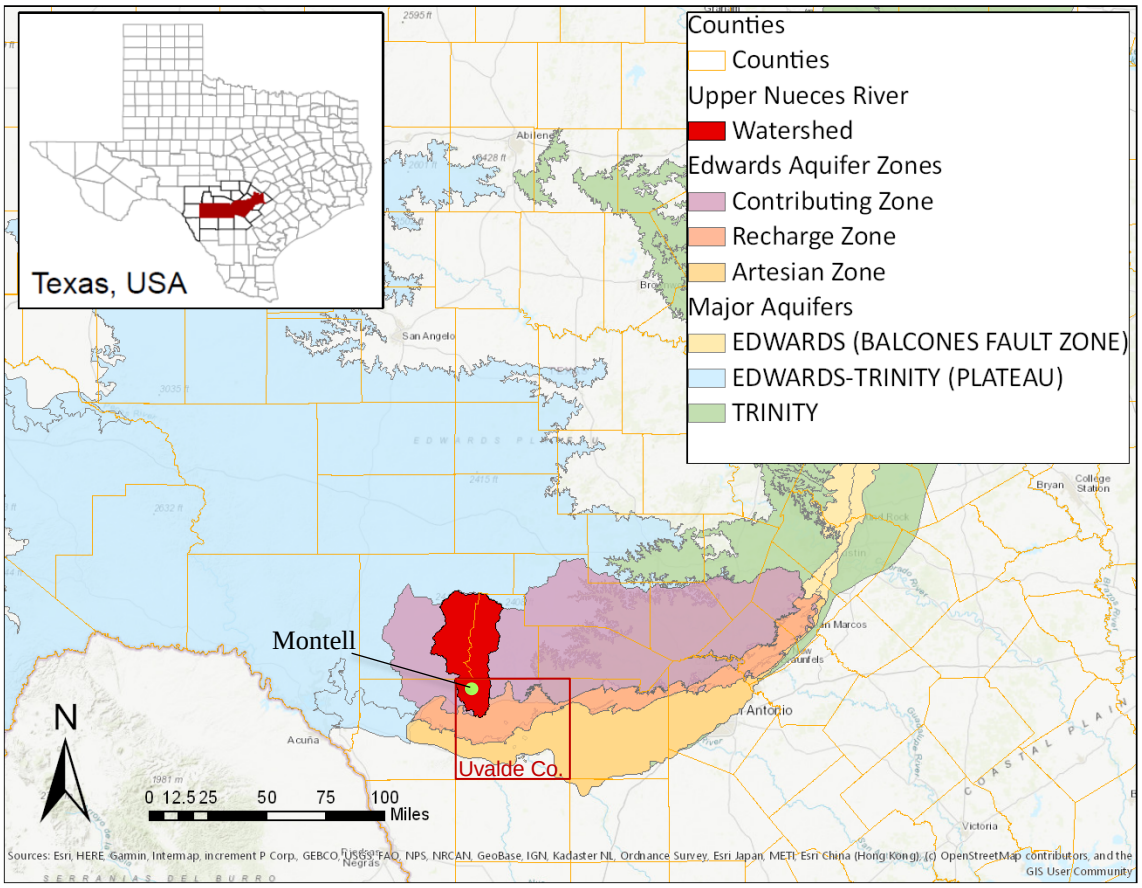

Figure 1. The upper Nueces River basin extends from Edwards and Real Counties downstream to the outcrop of Edwards Group limestone of the Edwards Aquifer Recharge Zone in Uvalde County. The upper basin is part of the Edwards-Trinity (Plateau) Aquifer and also the Edwards Aquifer Contributing Zone. (Adapted from EAA, 2017.)

Background

Study Area

The Nueces River is a 16,950 square mile (43,900 km^2) basin in south-central Texas, originating in Edwards and Real counties and flowing 315 miles (507 km) southeast to Corpus Christi Bay on the Gulf of Mexico. It is the westernmost basin draining the

Edwards Plateau. The upper Nueces River is defined here as the portion of the basin north and upstream of the Edwards Group outcrop in Uvalde County (Edwards Aquifer Contributing Zone, Figure 1). This region covers 2,152 square miles (5,574 km^2) and is part of the Edwards-Trinity (Plateau) Aquifer. The area is rural and hilly, with an approximately 1,000-foot (305 m) decrease in elevation from the Nueces headwaters to the flatter reaches downstream in Uvalde County. The climate of the upper Nueces basin varies from subtropical steppe to subtropical subhumid (Larkin and Bomar, 1983), with average rainfall of 23 in (58 cm). Precipitation is bimodal, with the greatest rainfall occurring from May — June and August — October, though storms with daily rainfall of 1 inch or greater can occur at any time of year (Larkin and Bomar, 1983).

Extremes in river discharge are characteristic of the Nueces River (Gustavson, 1978). Average summer (May 1 – August 31) stream discharge at U.S. Geological Survey (USGS) gage 08189998 (site name NUE020 in this paper, Figure 2) within the study area varies from over 200 cubic feet per second (cfs) (6 m^3/s) in a wet year (2015) to less than 5 cfs (0.1 m^3/s) in dry years (2011, 2013). Extreme drought occurred in the Nueces basin in 2011, when streamflow at the USGS gage was zero for five months between June and November. Between 01/08/2011 and 01/08/2018, streamflow exceeded 500 cfs (14 m^3/s) on five occasions, with storm events resulting in maximum discharge of over 1,000 cfs (28 m^3/s) in 2015 and 2016. Streamflow gains and losses within the study area have been documented in several previous studies, especially those conducted by the USGS and

Texas Water Board of Engineers (now called Texas Water Development Board). These are documented in Slade et al. (2002), Banta et al. (2012), and Kromann (2015).

There are significant gaining and losing reaches of the Nueces River in the upper basin near the small town of Montell, TX. This rural area is mostly rangeland with some irrigated fields but no direct withdrawals from the river. Candelaria Creek is a spring-fed tributary in Montell with a discharge of 25 – 40 cfs (0.7 – 1.1 m^3/s) in non-drought years (Figure 2). In drought conditions, the Nueces River can have zero flow upstream of the confluence with Candelaria Creek, and in such cases the creek comprises 100% of the Nueces River flow downstream of the confluence. Prolific springs are not unusual in this part of the Edwards Plateau (Brune, 1978). However, most springs originate at the contact between the Edwards and Trinity Limestone (George et al., 2011), whereas Candelaria Creek has incised approximately 100 ft (30 m) into the Upper Glen Rose (Trinity Group) Limestone. The origin of the creek's springflow is a major part of this study, and the results are upscaled to generate a conceptual model of the upper Nueces River basin. Using isotopic, specific conductance, and temperature data, Kromann (2015) estimated that Candelaria Creek's three springs (from north to south called Headwater, Middle, and South Springs) are sourced 80% from the Nueces River and 20% from the Trinity Aquifer. However, Kromann did not distinguish between groundwater sourced from the karstic Edwards-Trinity (Plateau) Aquifer and the overlying alluvial aquifer. This study further investigates the connection between the springs, local subsurface flowpaths originating from the Nueces River, and older groundwater draining from alluvial hillslopes.

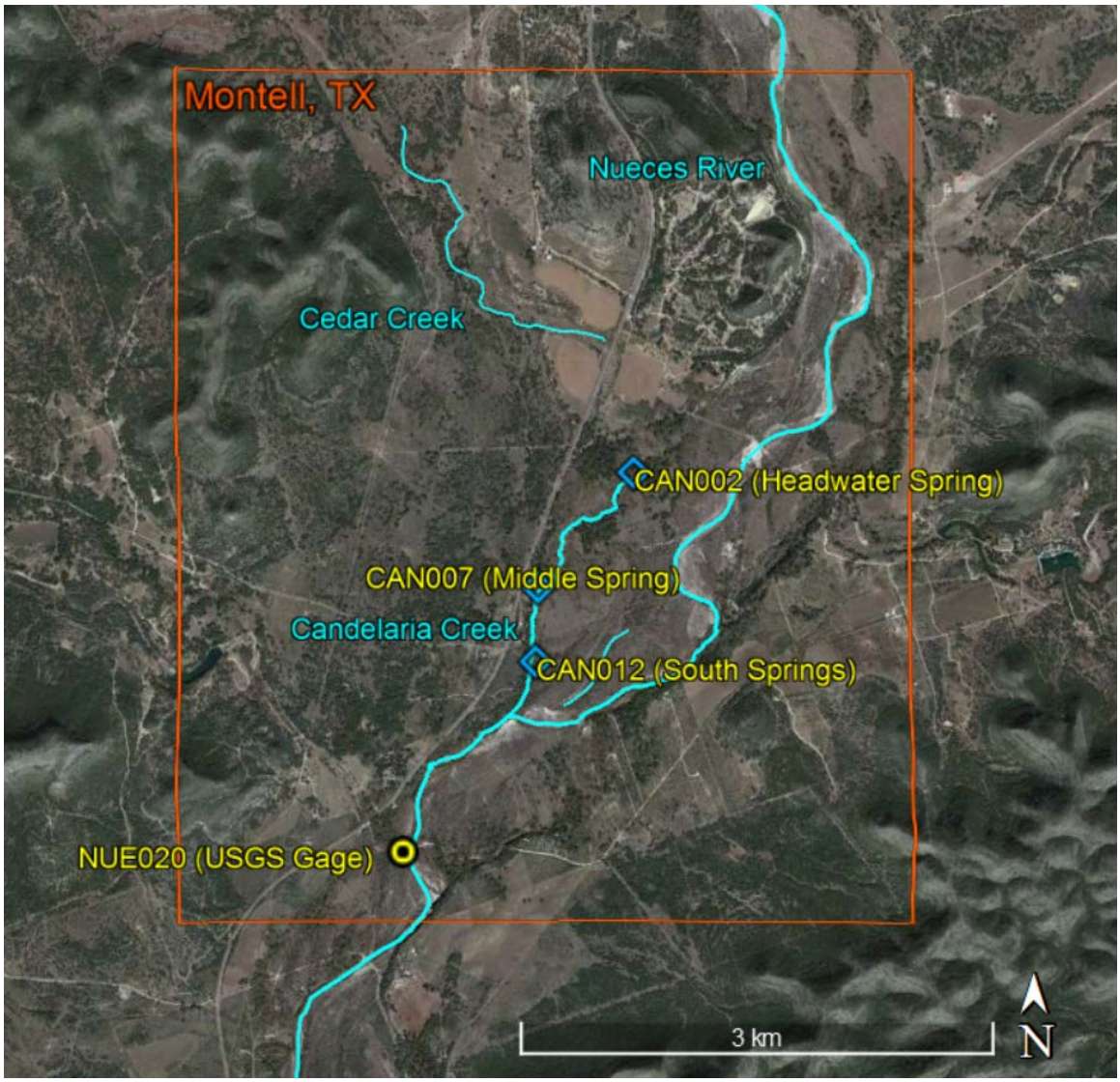

Figure 2. Candelaria Creek is a significant tributary to the Nueces River near the town of Montell, TX. The creek's three major springs are sourced from a combination of river water and alluvial groundwater, as first described by Kromann (2015).

Geology and Hydrogeology

The Edwards Aquifer is actually an aquifer system, which can be divided into three provinces: the Edwards (Balcones Fault Zone) Aquifer, the Edwards-Trinity (Plateau) Aquifer, and the Edwards (Washita Prairies) Aquifer (Sharp et al., 2019). The Edwards (Balcones Fault Zone) Aquifer is often colloquially referred to as the 'Edwards Aquifer', and the Edwards Aquifer Contributing Zone, Recharge Zone, and Artesian Zone all refer to the Edwards (Balcones Fault Zone) Aquifer. The Edwards Aquifer Recharge Zone (EARZ) is the region of the Edwards Plateau in which the Edwards Group crops out and surface streams are generally losing. Further south is the Edwards Aquifer Artesian Zone, where the Edwards Group is downdip and confined. Upstream of the EARZ is the Edwards Aquifer Contributing Zone (EACZ), where the Trinity Group crops out and Edwards Group limestone are found at higher elevations. Streams that drain the EACZ contribute allogenic recharge downstream where they cross the EARZ.

The study site is located in the upper Nueces River basin within the Devils River trend and Maverick Basin region of the Edwards-Trinity (Plateau) Aquifer, which corresponds with the EACZ of the Edwards Aquifer (Figure 3). The Edwards-Trinity (Plateau) Aquifer is mostly under water table (unconfined) conditions in the study area, and the base of the aquifer slopes to the south-southeast (Anaya et al., 2016). The Edwards Group limestone in the Devils River trend is of Lower Cretaceous age, and is overlain by the Del Rio Clay and underlain by the Upper Glen Rose limestone, considered to be the lower confining unit. Within the Devils River trend, the Edwards Group consists of the

Devils River Limestone, a 450-foot (137 m) thick complex formation of marine and supratidal deposits in the lower part and reefal or inter-reefal deposits in the upper portion (Maclay and Small, 1986). The Trinity Aquifer is composed of three permeable zones separated by two aquitards. The Upper Glen Rose Limestone is the upper zone, while the middle zone consists of the Lower Glen Rose Limestone, the Hensel Sand, and the Cow Creek Limestone. The lower zone consists of the Sycamore Sand, Sligo, and Hosston formations. The Upper Glen Rose Limestone is over 800 ft (244 m) thick and is yellowish-tan, thinly-bedded limestone and marl. It has a stair-step topography and can be identified in the field by its tan mudstones. It has mostly non-fabric selective porosity and generally has low permeability (Clark, 2003). In its furthest upstream reaches, the upper Nueces River channel has downcut into the Fort Terrett and Segovia formations of the Edwards Group (USGS, 2012). In the middle and lower reaches of the upper basin, the Nueces streambed is the Upper Glen Rose Limestone of the Trinity Group and hilltops consist mainly of Devils River Limestone (Edwards Group).

Several springs in the northern area of the upper basin appear in the Texas Water Development Board's *Major and Historical Springs of Texas* report (Brune, 1975). Springflow generally is sourced from the contact between the Edwards and Trinity group formations, often emerging at faults (Brune, 1975; George et al., 2011). Where alluvial units are present, springflow originates from the alluvial aquifer or is sourced from river underflow through bank deposits. Camp Wood Springs issues from alluvium but is sourced

from the Glen Rose limestone (Brune, 1981). The spring discharge is sufficient to supply municipal drinking water for the town of about 700 people.

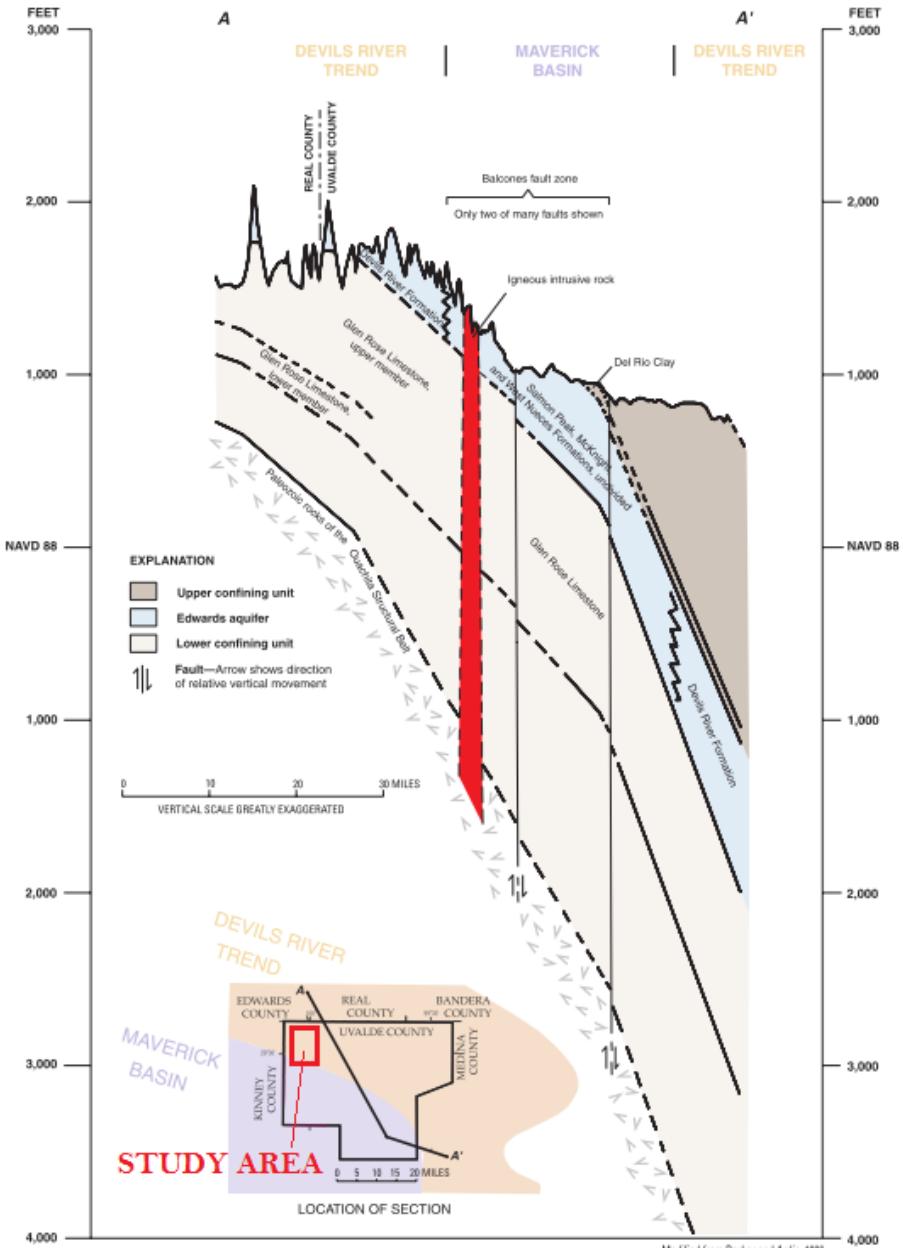

Figure 3. Stratigraphy of the upper Nueces River basin. Adapted from Clark (2003).

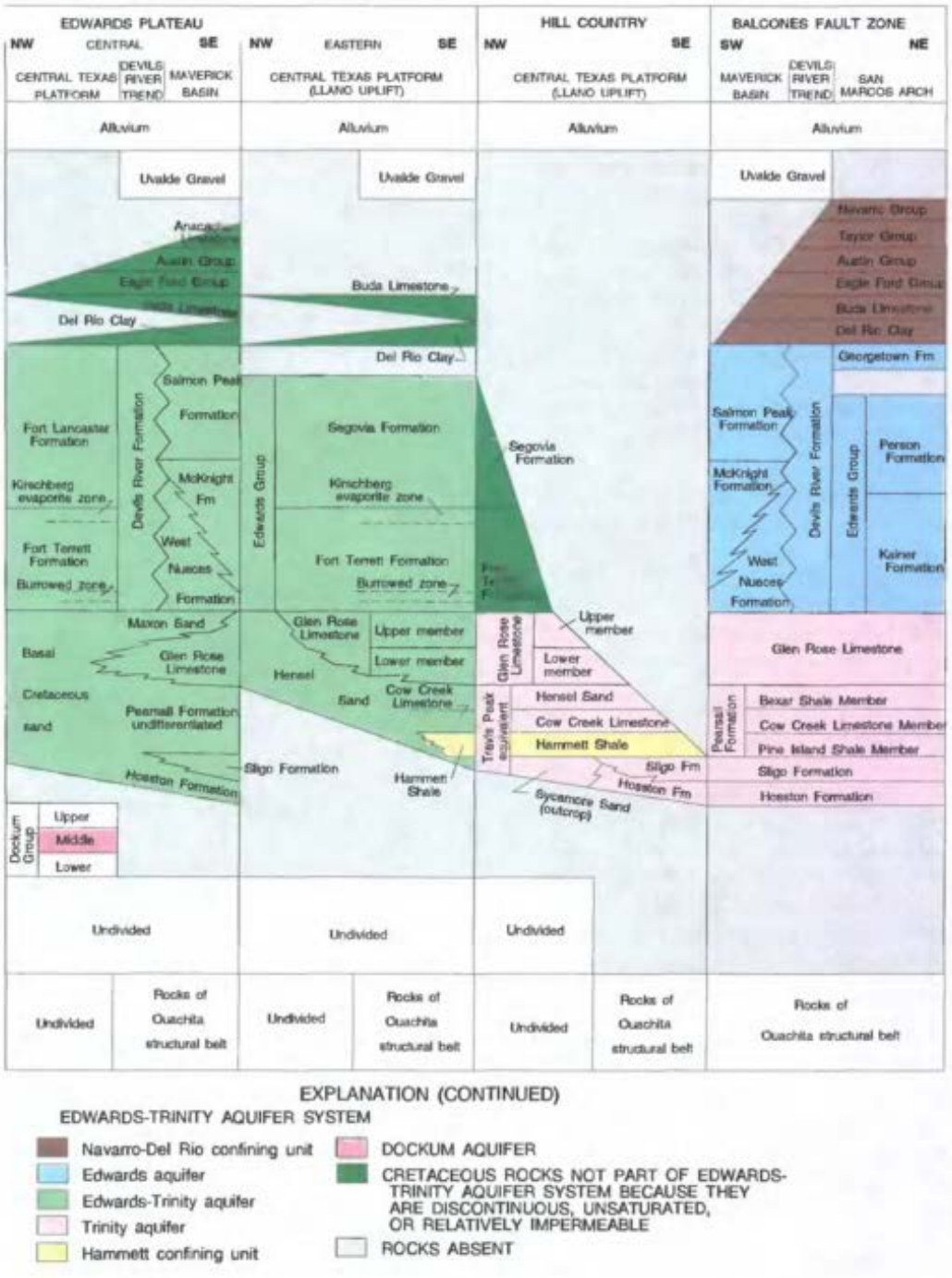

Figure 4. Stratigraphic units of the Edwards Aquifer System across the Edwards Plateau. From Barker et al., 1994.

ALLUVIUM-MANTLED KARST SYSTEM

The only river floodplain alluvial system recognized as an aquifer in Texas is the Brazos River Alluvium Aquifer (George et al., 2011), which has been studied extensively by researchers and agencies such as the USGS and Texas Water Development Board (TWDB). Sharp (1988) describes major floodplain alluvial aquifers as having valleys with thick, productive deposits that occur in a clearly defined band and are in contact with the river. Generally, rivers within major alluvial systems are gaining over the water year, and the potentiometric surface within the alluvium is slightly higher than the average river level (Sharp, 1988). For the most part, such rivers only partially penetrate their alluvial aquifers. The upper Nueces River alluvial aquifer has a depth and lateral extent that are at least an order of magnitude smaller than those of the Brazos or Mississippi River alluvial systems (Figure 5). Additionally, the Nueces River fully penetrates the alluvial aquifer; the river incises the Glen Rose Limestone of the floodplain floor. Although the upper Nueces River alluvial aquifer is not a major alluvial aquifer, there is reason to suspect that it has significant storage and yield.

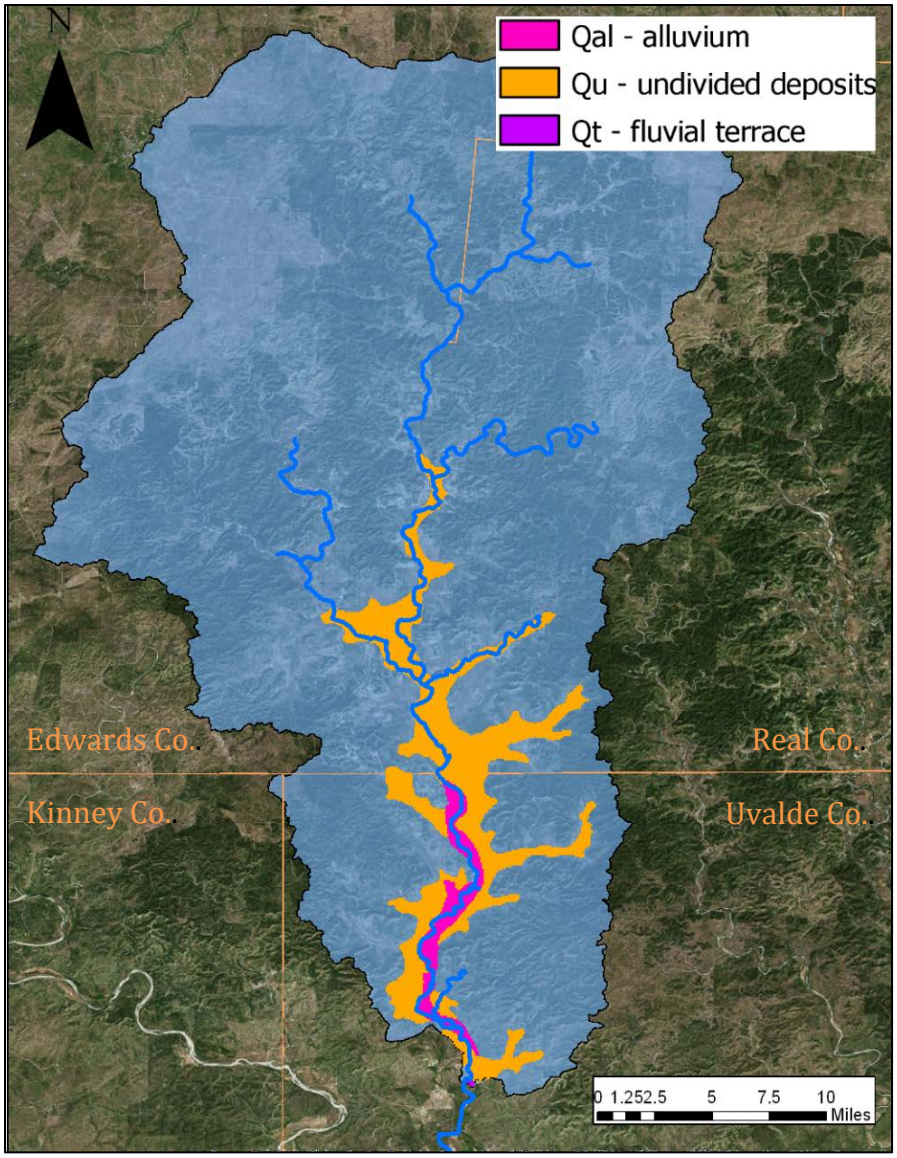

Figure 5. Alluvial units within the upper Nueces River basin (modified from the Geologic Atlas of Texas, Texas Natural Resources Information System).

The Nueces floodplain can be conceptualized as a floodplain conveyance system, a model suggested by Green et al. (2006) to describe the Leona River, also located on the Edwards Plateau (Texas). A floodplain conveyance system transports flow as surface water

in river and stream channels; groundwater through fluvial sediments of the alluvial aquifer; and groundwater through karst conduits in the underlying Glen Rose. Surface water and shallow groundwater exchange in alluvial deposits and terraces and emerge again as springflow. Woodruff and Abbott (1979) describe how karst conduits may be more prevalent in the shallow subsurface below floodplain channels through a positive feedback loop of development of preferential flowpaths under increased flow conditions. At some lateral distance away from the stream channel, bedrock no longer actively transports groundwater as part of the floodplain conveyance system. Although near-surface karst flow likely occurs, the approximate average depth to water in domestic wells in the Edwards-Trinity (Plateau) Aquifer in the upper basin is 110 ft (34 m), as determined from historical well logs (TWDB Groundwater Database, n.d.).

The upper Nueces River has a bedrock-alluvium channel with extensive deposits of Quaternary-age sediments mantling the upper member of the Glen Rose Limestone of the Trinity Group (Figure 6). Alluvium in and adjacent to the Nueces channel is composed primarily of chert cobbles in deposits up to 20 ft thick (6 m). As determined from well logs reported by the TWDB (TWDB Groundwater Database, n.d.), the broad floodplain terraces are topped by 2—8 ft (0.6—2 m) of top soil overlaying alternating lenses of clay, sandy clay, sandy loam, and gravel. Caliche can occasionally be found in deposits up to 20 ft (6 m) thick. Below these deposits is the gravel layer ranging from 10—40 ft thick (3—12 m), generally increasing in thickness from north to south in the basin. The TWDB classifies wells in the alluvium terraces within the study area as sourced from the 1212UVLD Uvalde

Gravel and the 100ALVM Alluvium. In well logs, the gravel unit is often classified as Leona Gravel (or Leona Formation) and occasionally as Uvalde Gravel.

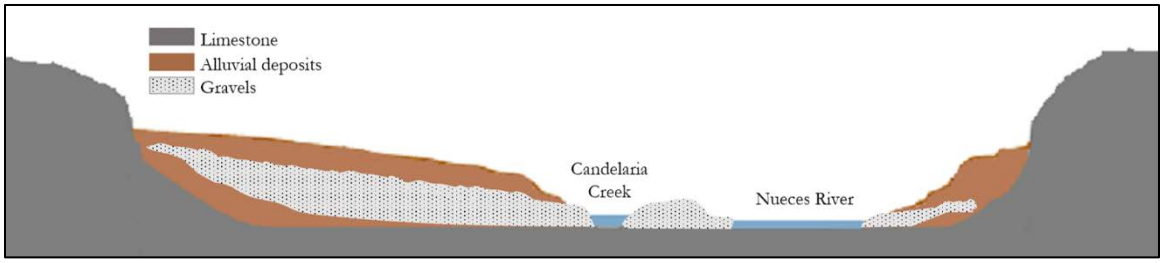

Figure 6. The Nueces River floodplain developed as streams incised into the Edwards and Trinity limestones. The Devils River Formation persists on some hilltops in the study area, and fluvial sediments mantle the Upper Glen Rose limestone of the Trinity Group. (Conceptual diagram; not to scale.)

Deposits of the Leona Formation are widespread across the Edwards Plateau and its margins. The Leona Formation is Pleistocene age and composed of fluvial gravel, sand, silt, and clay resulting from erosion of the Cretaceous carbonates of the Edwards Plateau (Barnes, 1974). Hemphill (2005) notes that the Leona aquifer in floodplains to the east of the Nueces basin may be unsaturated where drained by permeable bedrock. Historically, the names Leona Formation and Uvalde Gravels have been used to describe the same type of deposits. The Uvalde Gravel is Pliocene age and composed of caliche-cemented gravel, well-rounded chert cobbles, and some cobbles of limestone, quartz, and igneous rocks (Barnes, 1977). It was deposited by streams carrying sediments from the Edwards Plateau or from the High Plains farther northwest. Those streams were not preserved as the modern drainage system, and the Uvalde Formation was dissected by younger streams as base level dropped. The Leona Gravel was deposited in the newer stream valleys and is now dissected

by modern streams (Hemphill, 2005). When both units are present, they are distinguished by their topographic position. Generally, the Uvalde Gravel is located higher in valley topography than the Leona Gravel. The two formations are difficult to distinguish within the study area, which generally has only one unit preserved. Thus, neither name will be used here to refer to the mantled gravel in the upper Nueces basin. Additionally, recent alluvium is not always distinguished from the Leona Formation in the literature; here, 'recent alluvium' refers to chert gravels within and immediately adjacent to the Nueces channel that are younger than the alluvial terraces.

DYNAMIC RIVER LOSSES WITHIN THE EDWARDS AQUIFER CONTRIBUTING ZONE

Gain-loss surveys were conducted by Banta et al. (2012) for the U.S. Geological Survey (USGS) in 2008, 2009, and 2010 within the entire upper Nueces basin; the measurements reveal alternating gaining and losing reaches which vary with sampling date (Figure 7 and Table 1). (Site numbers generally increase from upstream to downstream.) July 2008 is considered to be a low-flow period and August 2009 was a very low-flow period. 2010 was a medium-flow period, and had slightly fewer losing reaches. As the gain-loss surveys were conducted under different climatic conditions, the absolute magnitudes of the discharge gains and losses cannot be directly compared. Patterns of gain-loss are dynamic in some reaches between successive surveys. Consistent streamflow loss occurs between the towns of Camp Wood (Figure 7, sites 28-30) and Montell (site 32, map inset). The river gains significantly between Montell and the town of Laguna (site 33 in Figure 7,

USGS gage site ID 08190000), which is located at the boundary between the recharge and contributing zones.

Kromann (2015) measured discharge at sites in Montell, TX, and to the south within the EARZ in 2012, 2013, and 2014, which were all low-flow or medium-flow periods. Her measurements reveal similar gain-loss patterns around Montell, with the largest magnitude loss occurring between NUE010 and NUE020 in all three surveys. Between NUE020 and site NUE060, which was Kromann's southernmost site within the EACZ, the river is overall gaining in the three surveys. Small losses of less than one cfs (0.03 m^3/s), reported by Kromann as indicating losing reaches, are within measurement uncertainty for stream gaging. Therefore it cannot be concluded that these reaches have actual losses. Within the EACZ, the sum of the measured gains and the sum of the measured losses between survey points are virtually equal in the 2012 and 2013 surveys. The sum of the streamflow gains is larger than the sum of losses in the EACZ in the 2014 survey.

Gary and Kromann (2013) studied the measured diurnal discharge fluctuations in the upper Nueces River. The average diurnal fluctuation ranged from 4 cfs (0.11 m^3/s) in summer 1994 to as high as 15 cfs (0.42 m^3/s) in January 2012; the lowest daily discharge typically occurred around 18:00hr (6:00PM) in summer months (Gary and Kromann, 2013). Several types of field data were collected to investigate whether the discharge fluctuations were primarily due to the invasive reed species *Arundo donax*, which colonized the upper Nueces basin in 2010 - 2011. No conclusion could be drawn from the field data, which were also collected after the removal of the majority of *A. donax*. The

measured discharge at sites in the study area of this investigation still had diurnal fluctuations over the monitoring period (January – November 2017).

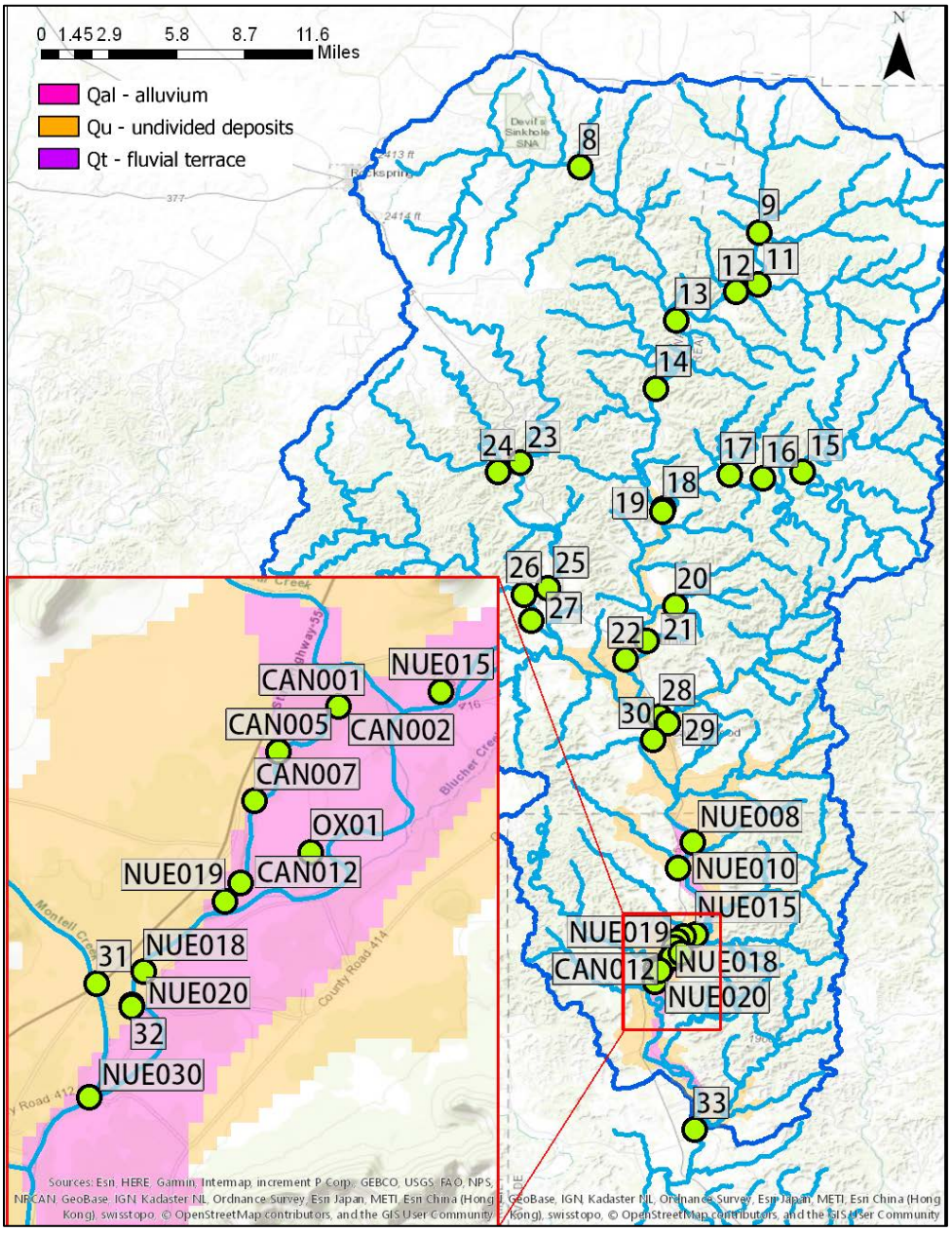

Figure 7. Approximate locations of previous gain-loss discharge surveys by Banta et al. (2012) and Kromann (2015). Table 1 lists discharge measurements at these sites.

Table 1. Results of gain-loss discharge surveys by Banta et al. (2012) for the U.S. Geological Survey and Kromann (2015).

	Measured Discharge (cfs)					
Site	**July 2008**	**August 2009**	**March 2010**	**January 2012**	**March 2013**	**March 2014**
8	0.73	1.96	0.19	-	-	-
9	-	5.48	6.81	-	-	-
11	-	1.44	-	-	-	-
12	11.6	7.12	-	-	-	-
13	13.3	9.63	15.4	-	-	-
14	12.4	-	7.2	-	-	-
15	-	0.42	-	-	-	-
16	-	0.68	0.91	-	-	-
17	1.89	1.7	4.9	-	-	-
18	0	3.79	-	-	-	-
19	9.12	2.19	-	-	-	-
20	-	0.57	-	-	-	-
21	14.8	2.64	36.9	-	-	-
22	-	16	50	-	-	-
23	0	0	-	-	-	-
24	4.56	1.17	-	-	-	-
25	-	0	5.48	-	-	-
26	0.67	0	2.7	-	-	-
27	2.85	-	6.69	-	-	-
28	0	-	-	-	-	-
29	-	-	2.49	-	-	-
30	34.7	-	79.7	-	-	-
NUE008	-	-	-	-	-	25.61
NUE010	-	-	-	32.39	26.36	30.48
CAN012	-	-	-	-	-	16.63
NUE020	-	-	-	10.36	8.66	11.62
31	0	-	-	-	-	-
32	12.4	0.71	-	-	-	-
NUE030	-	-	-	18.47	12.57	17.22
NUE040	-	-	-	17.68	16.29	22.81
NUE050	-	-	-	25.53	16.66	21.88
33	31	20	98	32.64	29.0	32.16

2. METHODS

To characterize shallow subsurface flow directions and velocities between the Nueces River and Candelaria Creek, gain-loss surveys, dye tracer testing, and groundwater depth measurements were used. Hydrograph analyses and floodplain mass balances were applied to calculate groundwater discharge to the Nueces River and the drainage rate of event water from bank storage. The intensive local observations were scaled up to characterize the hydrologic functions of the upper Nueces River basin alluvial aquifer.

The Nueces River sites used in this study are labeled from NUE010 at the upstream end and increasing in number up to NUE030 at the downstream end of the study area (Figure 8). NUE010 is the upstream control point for discharge gain-loss surveys, with a stream gage and a weather station maintained by the Edwards Aquifer Authority. It is also an injection site for tracer tests. NUE015 is roughly laterally even with the Headwater Spring of Candelaria Creek, site CAN002. CAN012 is a stream gage site located 50 m upstream of the confluence of the creek with the Nueces River. NUE018 is sited on the Nueces River just upstream of the Candelaria Creek confluence, and thus is used to measure the impact of inflows from the creek. During this study, discharge was always greater than zero at sites NUE015 and NUE018, but the river reach between the sites was completely dry during some periods of summer 2017. NUE020 is the location of USGS gage 08189998 that records precipitation and river stage.

Additionally, historic well logs from the TWDB Groundwater database were used to investigate lithology (particularly the depth and thickness of alluvial deposits) and

relative groundwater depths (in both the alluvial and bedrock aquifers). Data in the well logs were collected in different years under various hydrologic conditions. However, in the absence of other groundwater data, the well logs are used to give a rough approximation of the conditions in the upper Nueces River basin.

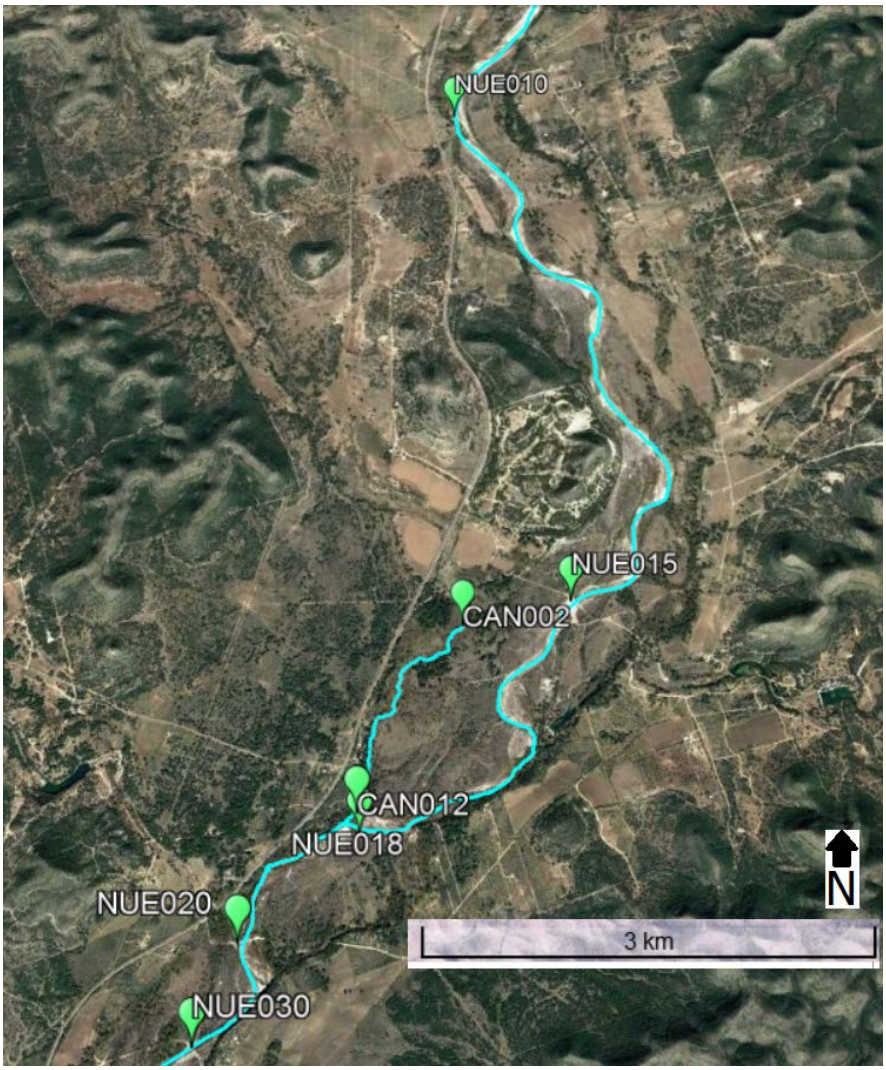

Figure 8. Main measurement sites within the study area. Site numbers increase from upstream to downstream.

Hydrograph Analyses

DISCHARGE GAIN-LOSS SURVEYS

Discharge gain-loss surveys consist of multiple discharge measurements to delineate stream reaches that gain water due to surface or groundwater inputs, or lose water due to groundwater recharge or anthropogenic pumping/diversions. This is also called differential gaging and is used to infer recharge from the river into an aquifer or groundwater discharge into a river (Scanlon et al., 2002; McCallum et al, 2013). Within the study area, there are no known surface water diversions, and discharge measurement locations were chosen such that gains or losses are assumed to be primarily due to groundwater inputs or losses and were not the result of surface tributaries. The discharge measurement sites used in this study are within the river reach with the greatest streamflow losses identified by previous studies (Banta et al., 2012; Kromann, 2015) and were chosen to test the hypothesis that Nueces River discharge losses are at least partially supplying springflow to Candelaria Creek. Table 2 lists the rating curves used to convert measured stream stage, *h*, in feet to discharge, *Q*, in cubic feet per second.

Table 2. Rating curves used at each gage site (stream depth in feet and discharge in cubic feet per second).

Gage location	Rating curve
NUE010	$Q = 69.64h^{1.20}$
NUE020	$Q = 37.36h^{2.31}$
CAN012	$Q = 2.30h^{3.95}$

BASEFLOW RECESSIONS

Analyses of stream hydrographs can reveal the contributions of overland flow, interflow, direct precipitation, and baseflow. Baseflow is the portion of stream discharge derived from drainage of groundwater from storage in the watershed. A hydrograph recession is the decline in streamflow after a precipitation event, and it reflects the storage characteristics of the basin including drainage area, topography, soil type, and aquifer properties. Generally, a deep, highly permeable aquifer can sustain stream baseflow for a longer period than can a shallow or low-permeability aquifer. A storm hydrograph is analyzed by separating the baseflow from the overland flow component, also called quickflow, surface flow, or direct runoff. (Direct precipitation on the stream and interflow from the unsaturated zone to the stream are usually ignored.) There are many methods used to determine when the recession flow becomes representative of baseflow. The calculated baseflow varies greatly depending on the arbitrarily chosen technique, and thus baseflow separation is useful to compare relative contributions of groundwater but not actual magnitudes (Dingman, 2002).

The time until the end of the overland flow component can be estimated using an empirical equation for large watersheds

$$T^* = A^{0.2} \text{ or } T^* = 0.827A^{0.2} \quad (1)$$

where T^*, also called D, is the number of days from the hydrograph peak to the end of direct runoff, and A is the area of the drainage basin in square miles (left equation) or in square kilometers (right equation). The exponential constant depends upon hydrogeologic characteristics including topography, vegetation, roughness, etc. (Fetter, 1994). The

streamflow recession on a hydrograph can usually be fitted with an exponential decay equation of the form

$$Q = Q_0 K^t = Q_0 e^{-at} \quad (2)$$

where Q is the discharge at a time t days after a given initial discharge, Q_0. K is the recession index, which reflects the physical characteristics of the watershed. On a semi-logarithmic plot of discharge vs time, K is the slope of the line of best fit. The baseflow recession equation commonly uses the form on the right, where a is the recession constant of the basin ($days^{-1}$). Deviations from an ideal linear recession curve (on a semi-logarithmic plot) can occur when a stream is fully penetrating, or entrenched, in the aquifer; when vertical loss of groundwater occurs to an underlying leaky aquifer; or when there are evapotranspiration losses of groundwater (Singh, 1968).

The seasonal baseflow recessions were determined from the available data at the three gage sites in the study area: NUE010 (upstream end), NUE020 (downstream end), and CAN012 (terminus of Candelaria Creek). The baseflow recession in the summer dry season begins T^* days after the peak discharge of the last major precipitation event in the month of May or June. Generally, only minor rainfall events occur between June and the start of the wet season in September or October. The winter baseflow recession begins T^* days after the peak discharge of the last rain event in November or December. In some years, minor rain events occurred later during the winter dry season (roughly December to April), however, the general baseflow recession trend is still evident.

The baseflow contribution to the upper Nueces River is assumed to be from the alluvial aquifer, although some springflow in the basin is sourced from karst discharge from the Edwards-Trinity (Plateau) Aquifer, especially in the river's furthest upstream reaches. The alluvial aquifer is assumed to follow the Dupuit-Boussinesq aquifer model, in which the stream channel is fully penetrating an unconfined rectangular aquifer, bounded below by a horizontal impermeable layer (in this case, the Glen Rose) (Brutsaert and Nieber, 1977). Using the HYDRORECESSION Matlab toolbox created by Arciniega-Esparza et al. (2017), baseflow was extracted with the methodology proposed by Brutsaert and Nieber based on the relationship between discharge (Q) and the rate of decline of discharge over time (dQ/dt).

Fluorescent Dye Tracer Testing

Non-toxic, fluorescent dye tracer tests were used to identify the principal flowpaths of shallow groundwater and to characterize hydraulic properties of the floodplain alluvium. Two cycles of dye tracing were used to investigate the sources of water supplying Candelaria Creek. The first was conducted on 03/15/2017 (wet season) and the second on 08/14/2017 (dry season), to compare surface water-groundwater exchange under different basin conditions. In both tests, uranine dye was added to the Nueces River at site NUE010, approximately six river kilometers upstream of the Candelaria Creek headwaters (Figure 14). This was hypothesized to be a sufficient distance upstream to capture possible subsurface flowpaths to the springs that supply the

creek. The injection location is an exposed bedrock reach approximately 65 feet (20 m) wide with an average water depth of 2.5 feet (0.8 m) during the first test and one foot (0.3 m) during the second test.

During the second dye tracer test, two additional fluorescent dyes, phloxine B and eosin, were injected into two groundwater wells (LW1 and CW1) in an alluvial terrace northwest of the headwaters of Candelaria Creek (Figure 17). These wells were hypothesized to be sourced from groundwater draining from hillslopes to the west of the Nueces and potentially flowing towards the river and the headwaters of Candelaria Creek. Both wells are used to support large-scale irrigation operations. LW1 is drilled in alluvium (depth unknown) and has a 200 gallon-per-minute (0.45 cfs; 0.01 m^3/s) pumping capacity in wet conditions. CW1 is drilled 40 ft (12 m) deep in alluvium and can supply 750 gallons per minute (gpm) (1.7 cfs; 0.05 m^3/s) in wet periods and 150 gpm (0.3 cfs; 0.01 m^3/s) in dry conditions (anecdotal evidence from landowner). Driller's logs are extremely limited within the study area; however, it is estimated that wells LW1 and CW1 are completed in 30 - 50 ft (9 - 15 m) of alluvium above the Upper Glen Rose Limestone.

Dye tracer methodology used herein is based on the protocols of the Edwards Aquifer Authority. Uranine (sodium fluorescein) liquid dye was used for surface water injection in this study and was selected because of its nontoxicity, cost effectiveness, and ease of detection. Uranine dye (Acid Yellow 73) has a molecular weight of 376.27 and fluoresces at a wavelength of 493 nanometers (nm). Phloxine B (Acid Red 92) fluoresces at 538 nm and eosin (Acid Red 87) fluoresces at 518 nm. Because the dyes fluoresce at

distinct wavelengths, they can be used simultaneously during a tracer test to reveal flowpaths.

The objective of tracer testing in this region is to use a sufficient quantity of dye for detection at monitoring points, but not enough to be visibly apparent in a private or public water supply well. A reasonable target peak recovery concentration is 0.05 g/m^3 (50 μg/L or ppb). Volumes were calculated using an empirical equation developed by Worthington and Smart (2003) from 185 tracer tests between sinkholes and springs over distances between 30 m and 30 km and with tracer recovery times varying from two minutes to two months. The following empirical formula from Worthington and Smart (2003) was used:

$$M = 19(LQC)^{0.95} \quad (3)$$

where M is the mass of dye injected (g); Q is the output discharge (m^3/s); C is the peak recovery dye concentration (g/m^3); and L is the distance (m) between injection and recovery points.

During the first dye tracer test, 20 kg of uranine liquid dye (40% concentration) was added to the Nueces River at site NUE010. The second test took place during summer low flow conditions, and 6.6 kg of uranine was added at NUE010. Additionally, during the second test 1.03 kg of eosin and 0.98 kg of phloxine B liquid dyes (40% concentration) were injected into wells LW1 and CW1, respectively. Both wells were flushed with at least 1,000 gallons (4 m^3) of water after dye injection to encourage dye movement out of the well into the subsurface. The eosin monitoring well (LW2) was pumped at a rate of

approximately 5 gpm (0.01 cfs) to create a stronger hydraulic gradient between the injection and monitoring locations. The water pumped out of LW2 was used for the automatic sampler and charcoal packet samples at site LW2.

Three different types of water samples were used to test for the presence of dye. Automatic water samplers (autosamplers) were deployed to collect sets of 24 samples at programmed intervals during the study period. Charcoal receptors (also called charcoal detectors) were used to determine whether dye traveled to sites not monitored by autosamplers. Charcoal adsorbs dye from the water that passes through the receptor. It yields a time-integrated sample that, barring interference from other organic compounds, is a product of continuous sorption of dye whenever dye is present in water. At certain locations, only grab samples were used to sample for dye concentration. Charcoal receptors were also deployed one to three weeks before dye injection to measure natural background fluorescence in the waters.

Vials from autosamplers and grab samples required no preparation before analysis. Dye was extracted from the charcoal receptors by eluting the charcoal for one hour in a solution containing 95% of a 70% solution of 2-propanol in water and 5% sodium hydroxide. Laboratory analyses for presence of dye (both water samples and eluent) were performed using a Perkin Elmer LS50B Luminescence Spectrometer. Samples were analyzed using a synchronous scan and right-angle sampling geometry. The scan spanned 401 to 650 nm at 0.5 nm intervals, with a difference between excitation and emission wavelengths (delta lambda, $\Delta\lambda$) of 15 nm and emission and excitation slits set

at 6 nm. Results of the analysis are recorded in intensity units of the excitation wavelength. However, the maximum intensity of each sample is the sum of any dye present plus background fluorescence. Dye peaks were separated from background fluorescence by fitting the curves to the Pearson VII statistical function using Systat PeakFit® software. The difference between sample and background fluorescence is the net intensity. Net intensity measurements were converted to a concentration (ppb) using calibration curves determined from analyses of standards for the three dyes. The standards were prepared in the laboratory using dilutions to obtain known dye concentrations.

Groundwater Calculations

UPPER BASIN ALLUVIAL AQUIFER STORAGE

Total groundwater storage capacity in alluvium in the upper Nueces floodplain was calculated using well records and driller's logs stored in the TWDB Groundwater Database (TWDB Groundwater Database, n.d.). Over 50 logs for wells within the alluvium outcrop of the upper basin were evaluated based on their position within the floodplain, lithology, total well depth, and recorded groundwater depth at the time of drilling. There are no maintained groundwater monitoring wells within the upper Nueces basin (the geographically closest monitoring wells are in the Edwards Balcones Fault Zone Aquifer and in the Frio River basin, respectively, and are too dissimilar from the study site conditions to be used). A best estimate of average saturated thickness of alluvium was made with the available data from TWDB as the difference between the

depth to the base of the gravel layer, $h_{alluvium\ base}$, and the depth to water, h_{water} (Equation 4). The average volume of water in alluvium storage, V_{GW}, was calculated as the product of the area of productive alluvium outcrop ($A_{productive}$), the average saturated thickness of alluvium (h_{sat}), and a conservative specific yield (S_y) of 15% (Equation 5).

$$h_{sat} = h_{alluvium\ base} - h_{water} \quad (4)$$

$$V_{GW} = A_{productive} * h_{sat} * S_y \quad (5)$$

$$V_{Max\ GW} = A_{productive} * h_{alluvium} * S_y \quad (6)$$

Heath (1983) and Morris and Johnson (1967) report specific yield (S_y) of gravel as 19% and 21%, respectively. Dingman (2002) reports a minimum specific yield of coarse gravel of 13% and maximum of 25%, and a minimum S_y of 17% and maximum of 44% for medium gravel. The surface area of alluvial units in the upper Nueces basin was determined from the Texas Natural Resources Information System geologic map (TNRIS, 2016). The area of productive alluvium, $A_{productive}$, is arbitrarily defined as 70 percent of the total area of alluvium outcrop, to account for lensing and other effects that reduce the lateral continuity of the gravel deposits. The maximum alluvial groundwater capacity was calculated as the product of the area of productive alluvium outcrop, the average thickness of the gravel layer ($h_{alluvium}$), and the specific yield (Equation 6). This approach is based on the method applied in the *2011 Plateau Region Water Plan* submitted to the TWDB (LBG-Guyton, 2010).

FLOODPLAIN MASS BALANCE

A basic floodplain mass balance was used to test whether discharge losses from the Nueces River are held in storage in alluvium and/or become recharge into the underlying Glen Rose Limestone. The amount of river discharge stored within the floodplain between successive measurement surveys was calculated assuming that all of the measured discharge lost between NUE010 and NUE018 becomes subsurface flow through alluvium (instead of discrete recharge to the bedrock). The volume of the river discharge losses between successive surveys was compared to the estimated alluvial storage capacity in the local floodplain. If the volume of river discharge losses is greater than the alluvial floodplain storage capacity, then some of the discharge losses must become discrete recharge to bedrock. Conversely, if the alluvial storage capacity is greater than the volume of river discharge losses, it is possible that river losses could be stored and transported through alluvial deposits. This method gives a first-order estimate of the possibility of river losses becoming springflow on Candelaria Creek and/or directly recharging into bedrock.

The discharge measurements on 02/18/2017 and 07/18/2017 were used to calculate the volume of discharge losses from the Nueces River. The difference in measured discharge at NUE010 and NUE018 on 02/18/2017 was 50 cfs (Table 5). On 07/18/2017, the discharge lost between the two sites was 43 cfs. The discharge loss is assumed to decrease linearly from the 50 cfs on the first survey date to the 43 cfs of the next survey date. There is a total loss of 13,835 acre-feet (17.1×10^6 m^3) of river water over the 150 days between the surveys, or an average of 92 acre-feet per day (0.1×10^6

m^3/day). This calculation was repeated for the losses between NUE015 and NUE018: the river discharge lost between NUE015 and NUE018 was 20 cfs (0.6 m^3/s) on 02/18/2018 and 8 cfs (0.2 m^3/s) on 07/18/2018. The total river water lost over the 150 day period was 4,165 acre-feet (5.1 x 10^6 m^3), or an average loss of 28 acre-feet per day (35,000 m^3/day) within this reach. Average Candelaria Creek discharge in the same period was 64.6 acre-feet per day (80,000 m^3/day).

Four cross-sections, mapped in Figure 9 and shown in Figure 10, were used to estimate the volume of alluvium within the study area between sites NUE010 (upstream river measurement site) and NUE018 (just upstream of the confluence with Candelaria Creek). The cross-section surface elevations were derived from LiDAR datasets (StratMap 2014 50cm Bandera & Lampasas Lidar) from the Texas Natural Resources Information System. A simple floodplain geometry was assumed (similar to the conceptualization shown in Figure 6), with a generally flat bottom boundary of limestone bedrock at the elevation of the streambed, and alluvial terraces composed primarily of high-conductivity gravels.

The alluvial storage capacity for the floodplain reach between NUE010 and NUE018 was calculated with the same methodology of Equations 5 and 6. The thickness of the gravel layer ($h_{alluvium}$) was estimated for each cross-section according to the geometries shown in Figure 10. There are no accessible monitoring wells within the study area, so the saturated thickness of alluvium (h_{sat}) was estimated based on the LiDAR-derived topography and field observations of water levels. For the terrace between the

Nueces River and Candelaria Creek, the water surface elevation of an oxbow pond was assumed to reflect the water table elevation of the terrace. Again it was assumed that the alluvial aquifer has a specific yield, S_y, of 15 percent. The alluvial storage capacity was also calculated for the reach between NUE015 and NUE018 to isolate the importance of storage in and transmission through the terrace between the Nueces River and Candelaria Creek. Table 3 lists the estimated cross-sectional area of alluvium at each transect and the alluvium storage capacity of the floodplain between successive transects.

Table 3. Cross-sectional area of alluvium at the four floodplain transects and the storage capacity of the floodplain between transects. Water table depths in alluvium were estimated based on topography and field observations.

Transect	Cross-sectional area of alluvium (m^2)	Cross-sectional area of saturated alluvium (m^2)	Floodplain reach between transects	Total groundwater storage capacity (10^6 m^3)	Saturated storage (10^6 m^3)
NUE010	7,059	1,400	NUE010 – NUE012	4.29	1.08
NUE012	12,000	3,400	NUE012 – NUE015	3.38	0.66
NUE015	9,150	1,115	NUE015 – NUE018	2.03	0.35
NUE018	4,400	1,225	TOTAL (NUE010 – NUE018)	9.70	2.09

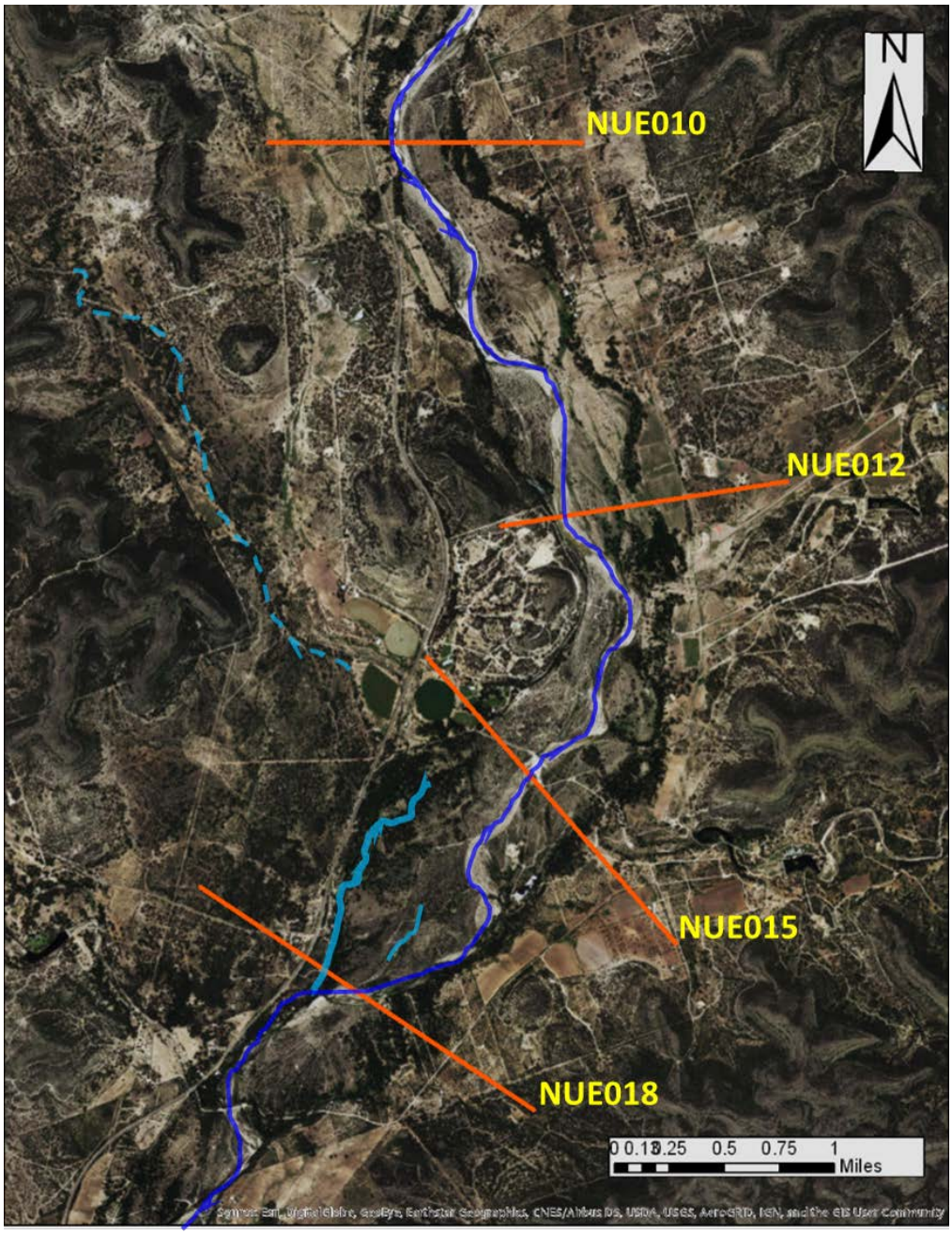

Figure 9. Location of floodplain cross-sections derived from LiDAR.

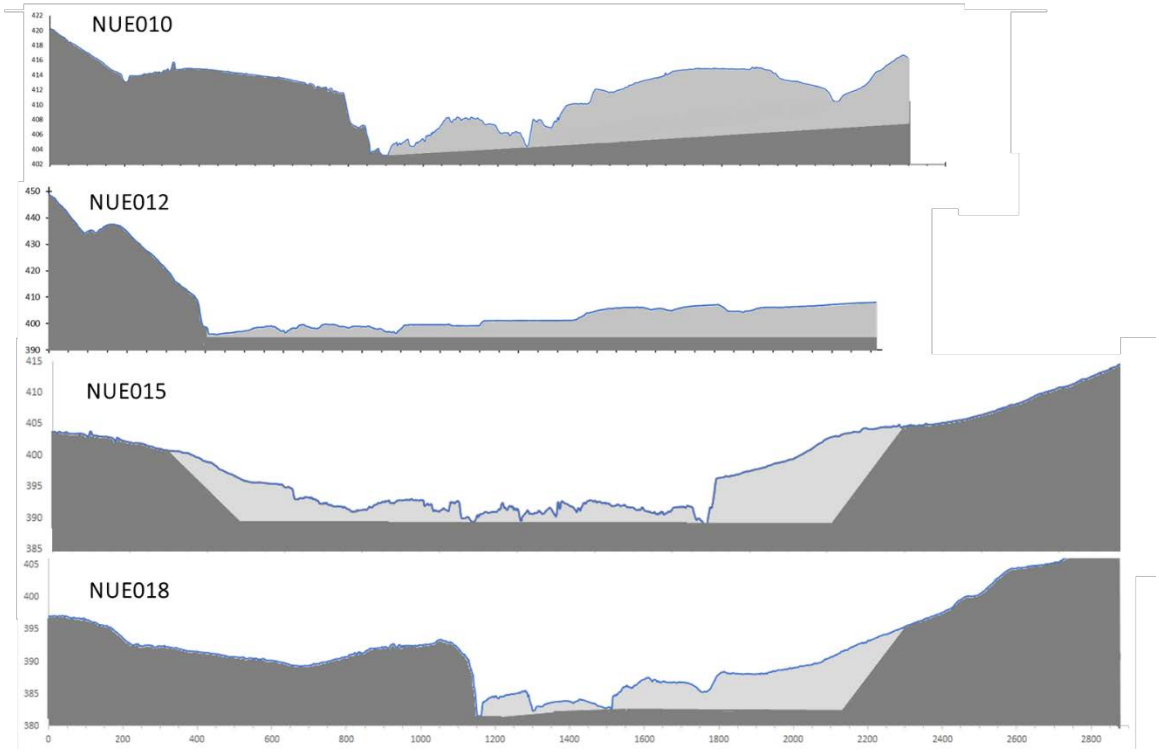

Figure 10. Floodplain cross-sections derived from LiDAR (cross-sections are of varying length; axes are shown in meters). Depth of bedrock (dark gray) is assumed equal to the streambed elevation in most cases. The volume of the alluvial aquifer (light gray) is approximated as shown based on topography and site observations.

BASEFLOW CONTRIBUTION OF THE ALLUVIAL AQUIFER

The USGS gage at the town of Laguna (USGS site number 08190000; site 33 in Figure 7) measures discharge as the Nueces River leaves the Contributing Zone and enters the Recharge Zone. The Laguna gage is the recharge index gage in the Nueces basin; discharge losses between the Laguna gage and the next downstream gage (south of Uvalde, TX) are considered to become recharge to the Edwards Aquifer. It is convenient to use the Laguna gage to summarize the effect of the alluvial aquifer in the upper Nueces River basin.

The alluvial aquifer is approximated as two linear reservoirs: one reservoir represents the relatively more consolidated alluvial terraces which are assumed to be located more than 75 m from the river, and the other reservoir is the unconsolidated alluvial deposits within 75 m of either side of the river axis. The variation in storage in the terrace portion of the alluvial aquifer has a longer timescale that is based on seasonal and year-to-year hydrologic conditions. Conversely, the storage and drainage rates of the near-river portion are assumed to vary proportionally to the stage height of the river.

The change in storage in the terrace reservoir of the alluvial aquifer is calculated as the product of surface area ($A_{productive}$), storativity (S), and change in head (Δh) (Equation 7). The terrace reservoir is the alluvial outcrop area that is more than 75 m from the axis of fourth- and fifth-order streams. The $A_{productive}$ of this reservoir is 79 km^2, which accounts for the area of productive alluvial outcrop (70% of total area). Storativity, S, is assumed to be 22%. The change in head, Δh, varies with the overall watershed conditions: 0.5 m/yr in the drought conditions of April 2011 – May 2015 and 1.5 m/yr in the wet watershed condition which began in May 2015. The period before April 2011 is assumed to have an intermediate hydrologic condition, with a change in head in the terrace reservoir of 0.75 m/yr. This estimation does not account for changes in outflow rate from this reservoir over the course of the year; the discharge of terrace alluvial groundwater is constant for each of the three hydrologic periods (intermediate, dry, wet).

$$\Delta V_{GW} = A_{productive} * S * \Delta h \quad (7)$$

The near-river reservoir of the alluvial aquifer in this simplified conceptualization is considered to be the alluvium within 75 m on either side of the fourth and fifth order streams in the upper basin, with a surface area of 18 km^2. In this case, the entire 18 km^2 surface area is assumed to be productive. Hydraulic conductivity (K_{sat}) is assumed to be 9.8 x 10^{-4} ft/s (3 x 10^{-4} m/s), which is reasonable based on field observations along the Nueces River. Discharge from the near-channel alluvium to the river, $Q_{GW,}$ is calculated using Darcy's law as the product of the hydraulic conductivity, hydraulic gradient (*i*), and the cross-sectional area perpendicular to the river (*A*) (Equation 8). The hydraulic gradient depends on the river depth at the Laguna gage, *h(t)*, and the hydrologic condition of the watershed (intermediate, dry, or wet), which determines the h_0, the hydraulic head at a distance Δx (75 m) from the river (Equation 9). The average hydraulic gradient (*i* or *dh/dl*, unitless) in near-channel alluvium is 3 x 10^{-4} over the drought period, 6 x 10^{-4} during the intermediate condition, and 3 x 10^{-3} in the recent wet period. Table 4 summarizes the parameters used in the near-river alluvial reservoir calculations.

$$Q_{GW} = K_{sat} * i * A \quad (8)$$

$$i = \frac{h_0 - h(t)}{\Delta x} \quad (9)$$

To assume that all flow is perpendicular to or from the river is a significant idealization. Alluvial aquifers can be dominated by flowpaths parallel to the floodplain longitudinal axis, called underflow, or by the baseflow component of groundwater flux, which is normal

to the river (Larkin and Sharp, 1992). In this simple model, the near-channel reservoir flux is entirely baseflow.

Table 4. Parameters for the calculation of the near-river alluvial reservoir contribution to Nueces River baseflow.

Hydrologic period	h_0 (ft / m)	Average hydraulic gradient (unitless)
Intermediate: January 2009 - April 2011	2.4 / 0.73	6×10^{-4}
Dry: April 2011 – May 2015	2.2 / 0.67	3×10^{-4}
Wet: May 2015 – April 2017	3.5 / 1.07	3×10^{-3}

3. RESULTS

REPRESENTATIVE WATERSHED REACH: CANDELARIA CREEK

The large streamflow loss around Montell, TX, was investigated with differential gaging conducted between January and December 2017, which was a relatively wet period within the upper basin. (Site names are labelled in increasing order from upstream to downstream.) Site NUE018 was added between NUE010 (upstream boundary of study area) and NUE020 (downstream boundary of study area) to isolate the effect of Candelaria Creek inflow. Results of the synoptic surveys are displayed in Figure 11 and listed in Table 5. The Nueces River consistently loses flow between site NUE010 and site NUE018, which

is just upstream of the confluence with Candelaria Creek. The losses from the Nueces cannot be explained by evapotranspiration alone (Gary and Kromann, 2013), and no pumping occurs from the river within the study area (although high-capacity irrigation wells are used within adjacent alluvial terraces). Streamflow losses are therefore assumed to be due to the vertical and lateral migration of water into unconsolidated gravel bars and banks or into discrete karst features or faults. The discharge lost between NUE010 and NUE015 is on average a 33% loss in normal/wet conditions (01/28/2017, 02/18/2017, 03/15/2017 surveys); a 68% loss in medium-flow conditions (11/05/2017 survey); and an average of 79% loss in low-flow conditions (07/18/2017 and 08/14/2017 surveys). The discharge lost between NUE015 and NUE018 ranged from 33% loss (02/18/2017) to 46% loss (07/18/2017) on the survey dates. However, in summer low-flow conditions, the river reach immediately downstream of NUE015 is often completely dry before regaining some flow upstream of NUE018.

Some or all of the river discharge lost between NUE010 and NUE018 may become springflow on Candelaria Creek, a major tributary that originates within an alluvial terrace. Discharge survey sites were added along the length of the creek to isolate the contributions from the three sets of springs that were identified. Candelaria Creek is a gaining stream over its entire length from the Headwater Spring (CAN002) downstream to its confluence with the Nueces River (downstream of site CAN012). An average of 20% of creek flow is generated between the headwaters (CAN002) and site CAN005 (streamflow surveys on 02/18/2017 and 07/18/2017). On average, 27% of streamflow is generated between

CAN005 and Middle Spring (CAN007), and 53% of creek flow is generated in the downstream half of the creek between CAN007 and CAN012. In the 2017 study period, Candelaria streamflow remained relatively constant while the Nueces streamflow declined by more than half during the summer months.

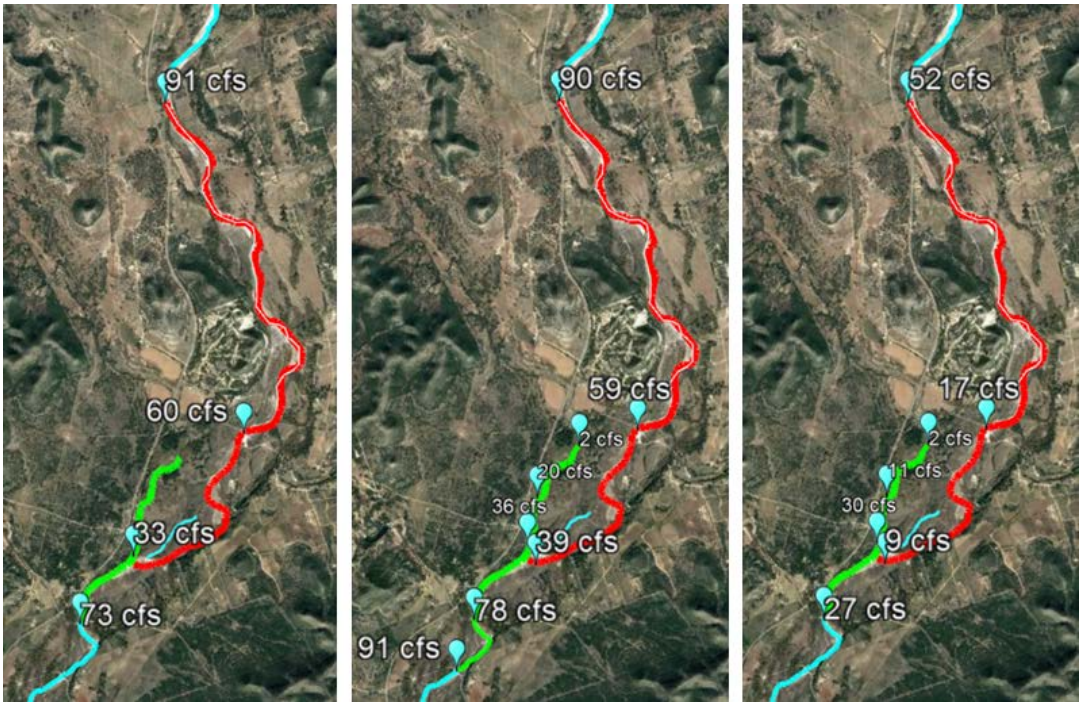

Figure 11. Results of synoptic gain-loss surveys conducted on 01/28/2017; 02/18/2017; and 07/18/2017 (left to right). Inflow from Candelaria Creek significantly restored river flow, especially in the summer season.

Table 5. Synoptic surface water discharge measurements completed within the study area in 2017. See Figure 6 for corresponding site locations.

Location of Discharge Measurement	Discharge (ft^3/s) by Date of Measurement						
	1/28/17	**2/18/17**	**3/15/17**	**6/13/17**	**7/18/17**	**8/14/17**	**11/5/17**
NUE010	91.3	90	101.8	112	52.3	40.03	67.5
NUE015	59.9	59.1	68.7	-	17	4.1	21.8
NUE018	-	39.4	-	-	9.1	-	-
NUE020	72.8	77.8	-	100	26.9	23.4	52.7
NUE030	-	91.3	100.1	-	-	-	-
CAN002	-	2.27	-	-	1.8	-	-
CAN005	-	6.35	-	-	6.5	-	-
CAN007	-	20	-	-	11.3	-	-
CAN012	33.2	35.5	37	37.5	29.6	23.2	33

STREAMFLOW IN DROUGHT VS. NORMAL CONDITIONS

Texas experienced the second-worst drought on record between 2010—2014. Three months of dry weather in late 2010 preceded the driest year on record in Texas in 2011. Statewide total rainfall was only 11 inches (28 cm) in the water year of October 2010—September 2011; average rainfall during the water year was 27 inches (69 cm) for the 1981-2010 period of record (TWDB, 2017 State Water Plan). Average annual rainfall is 27 inches (69 cm) in Edwards and Uvalde counties (upper Nueces basin). Below-average annual precipitation in the west Plateau and east Plateau regions was recorded in 2010—2015, although the trend toward low rainfall began around 2008.

The Nueces River flow near NUE020 was measured at only 0.71 cfs (0.03 m^3/s) in August 2009, and zero flow at site NUE020 was recorded from July 5—November 28, 2011. It was also dry from May 5—26, 2013 and July 25—October 7, 2013. Even in years

with significant spring precipitation, the Nueces River can have low to zero flow within the study area by late summer. At these times, input from Candelaria Creek accounts for 100% of Nueces River flow at site NUE020, such as during the 2017 summer dry period.

Candelaria Creek still flows even when the Nueces River loses all discharge (Kromann, 2015). The minimum discharge from Candelaria Creek in the period of record is 6 cfs (0.2 m^3/s), which occurred from September 3—October 19, 2013 and again from August 25—September 7, 2014. Average creek discharge for the water year October 2013—September 2014 was 15 cfs (0.4 m^3/s). Average creek discharge for water year 2016 - 2017, a relatively wet year, was 38 cfs (1 m^3/s), and the lowest creek flow in calendar years 2016—2017 was 20 cfs (0.6 m^3/s) on 06/14/2016.

Hydrologic Mass Balance

Discharge losses could become springflow in Candelaria Creek via diffuse flow in near-channel alluvial terraces or even as karst conduit flow. Surface water elevations derived from a digital elevation model (from LiDAR collected in 2014) reveal a hydraulic gradient that could drive subsurface flow from the Nueces River to Candelaria Creek within this reach (Figure 12). This gradient suggests that subsurface transport occurs through the alluvium rather than the bedrock underlying the deposits. Preliminary geophysical surveys (electrical resistivity, electromagnetic, and ground-penetrating radar) of the terrace between the river and creek support this hypothesis, as major conduits, faults, or other features were not found in the bedrock. The river reach between NUE010

and NUE018 has significant deposits of chert cobbles and gravels (Figure 13). It was hypothesized that the deposits provide a high conductivity flowpath from the Nueces River to Candelaria Creek when the river stage is high.

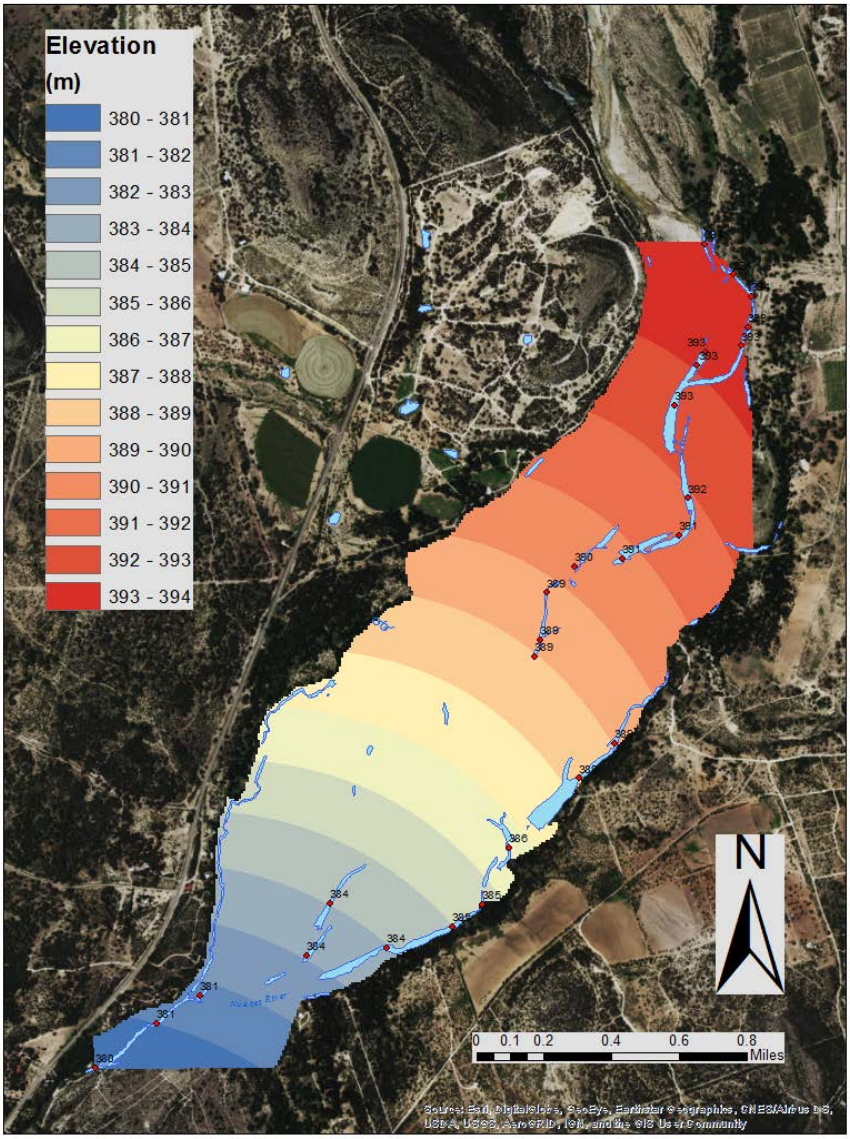

Figure 12. Surface water elevations derived from LiDAR reveal a hydraulic gradient that could drive subsurface flow of river water through alluvium to the downstream portion of Candelaria Creek (modified from Dr. Mark Helper, unpublished figure).

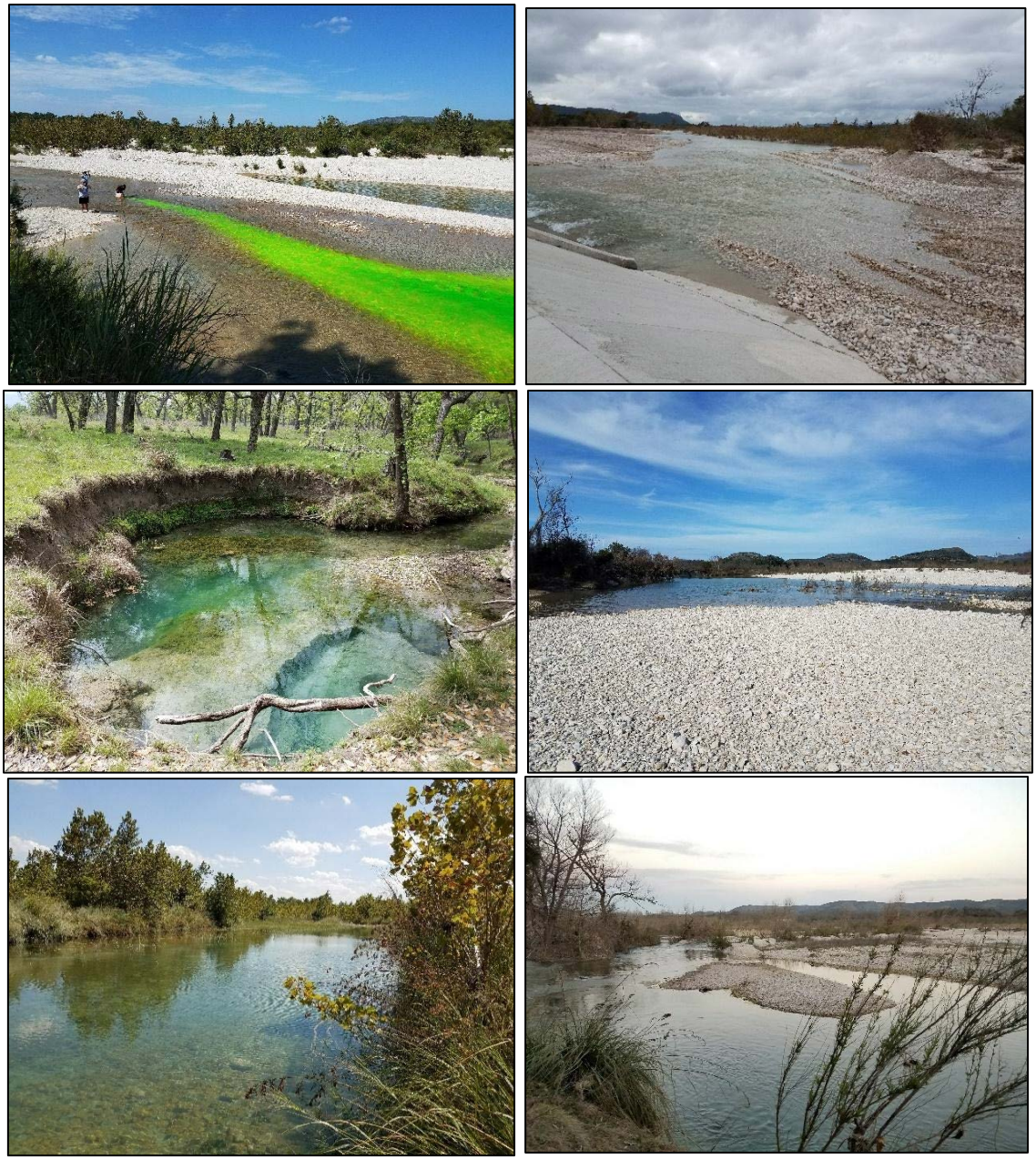

Figure 13. Top: Extensive gravel deposits at NUE010 on the date of the second tracer test (left) and at NUE015 (right). Middle: The Headwater Spring (CAN002) of Candelaria (left) and a broad gravel terrace at a site halfway between NUE015 and NUE018 (right). Bottom: The oxbow pond reflects the water table elevation of the terrace between the river and creek (left). Candelaria Creek, at left in the photograph, enters the Nueces River at NUE018 (right).

The river reach between NUE010 and NUE018 has an estimated maximum alluvial groundwater storage capacity of 7,867 acre-feet (9.7 x 10^6 m^3). The average saturated alluvial volume in the reach is 1,695 acre-feet (2.1 x 10^6 m^3), based on an estimated water table elevation using surface water elevations and floodplain topography. During the synoptic discharge survey on 02/18/2017, discharge lost between NUE010 and NUE018 was 50 cfs (1.4 m^3/s). On 07/18/2017, 43 cfs (1.2 m^3/s) of streamflow was lost between the sites. Total river discharge loss was 13,835 acre-feet (17.1 x 10^6 m^3) over the 150 days between surveys, with an average of 92 acre-feet per day (0.1 x 10^6 m^3/day). There is sufficient storage within the alluvial floodplain to store and transport the lost river discharge.

Discharge from Candelaria Creek (CAN012) was 35.5 cfs (1 m^3/s) on 02/18/2017 and 29.6 cfs (0.8 m^3/s) on 07/18/2017. Candelaria Creek discharged a total volume of 9,684 acre-feet (11.9 x 10^6 m^3) over the 150 days, with an average of 65 acre-feet per day (80,000 m^3/day). Assuming that the entire Candelaria Creek discharge is sourced from river underflow through alluvium, there are still 4,151 acre-feet (5.1 x 10^6 m^3) of lost river discharge that are unaccounted for in this mass balance over the 150-day period, or 28 acre-feet per day (35,000 m^3/day). This volume could be stored within the alluvial floodplain, or could become discrete recharge into the Glen Rose Limestone bedrock.

The reach between NUE015 and NUE018 was further examined to determine if the losses there could be entirely responsible for springflow on Candelaria Creek. The maximum groundwater storage capacity is 1,648 acre-feet (2 x 10^6 m^3) in this reach, and

the average actual groundwater storage is 285 acre-feet (0.4 x 10^6 m^3), based on surface water elevation in the oxbow pond. The river discharge lost between NUE015 and NUE018 was 20 cfs (0.6 m^3/s) on 02/18/2018 and 8 cfs (0.2 m^3/s) on 07/18/2018, which amounts to 4,165 acre-feet (5.1 x 10^6 m^3) over the 150-day study period, and an average loss of 28 acre-feet per day (35,000 m^3/day) within this reach. Candelaria Creek discharge was an average of 64.6 acre-feet per day (80,000 m^3/day) in the same period. There is enough capacity in the alluvium to transport the entirety of the discharge lost between sites NUE015 and NUE018. However, the discharge lost between NUE015 and NUE018 is not sufficient to be the sole source of Candelaria Creek springflow. Therefore the creek must be supplied in part by river losses upstream of site NUE015, or by alluvial groundwater from the terrace northwest of the creek.

Fluorescent Dye Tracer Testing

Fluorescent dye tracer tests were used to examine subsurface flowpaths and to test the hypothesized hydraulic connection between the Nueces River and Candelaria Creek. Uranine dye (also called sodium fluorescein) was injected into the Nueces River at site NUE010 to investigate the substantial streamflow losses between NUE010 and NUE018. Injection at NUE010 was repeated in high- and low-flow conditions to evaluate dynamic seasonal behavior of the floodplain. During the low-flow tracer test, two additional fluorescent dyes were injected into wells within the alluvial terrace north of the Candelaria

Creek headwaters. Figure 14 is a map of locations relevant to the first tracer test, and Figure 17 includes locations from the second tracer test.

RIVER UNDERFLOW THROUGH ALLUVIUM

The first fluorescent dye tracer test assessed potential subsurface flowpaths between the Nueces River and Candelaria Creek in the wet season. Uranine injection occurred at 17:20 on 03/15/2017 at NUE010 (Figure 15). An autosampler at site NUE015, 5.8 km downstream of the uranine dye injection site, recorded a breakthrough concentration of 5.3 ppb in a water sample at 01:00 on 03/16/2017 (Figure 15). A peak concentration of 100 ppb at NUE015 occurred five hours after dye breakthrough, and then diminished to less than 30 ppb over the next six hours. Samples had detectable dye levels through 03/20/2017 (after this date the autosampler was removed due to restricted access to the site). Water samples from the autosampler at NUE018, 9.2 km downstream of the injection site, first recorded a detectable amount of uranine at 06:00 on 03/16/2017. A peak concentration of 19 ppb occurred five hours later and dye remained detectable through 03/22/2017. The extended presence of dye in the river could be due to hyporheic exchange in the river banks and bed, which lengthen surface water flowpaths. The diminished peak dye concentration at NUE018 as compared to the peak at NUE015 suggests loss of dye to the subsurface through lateral and vertical exchange.

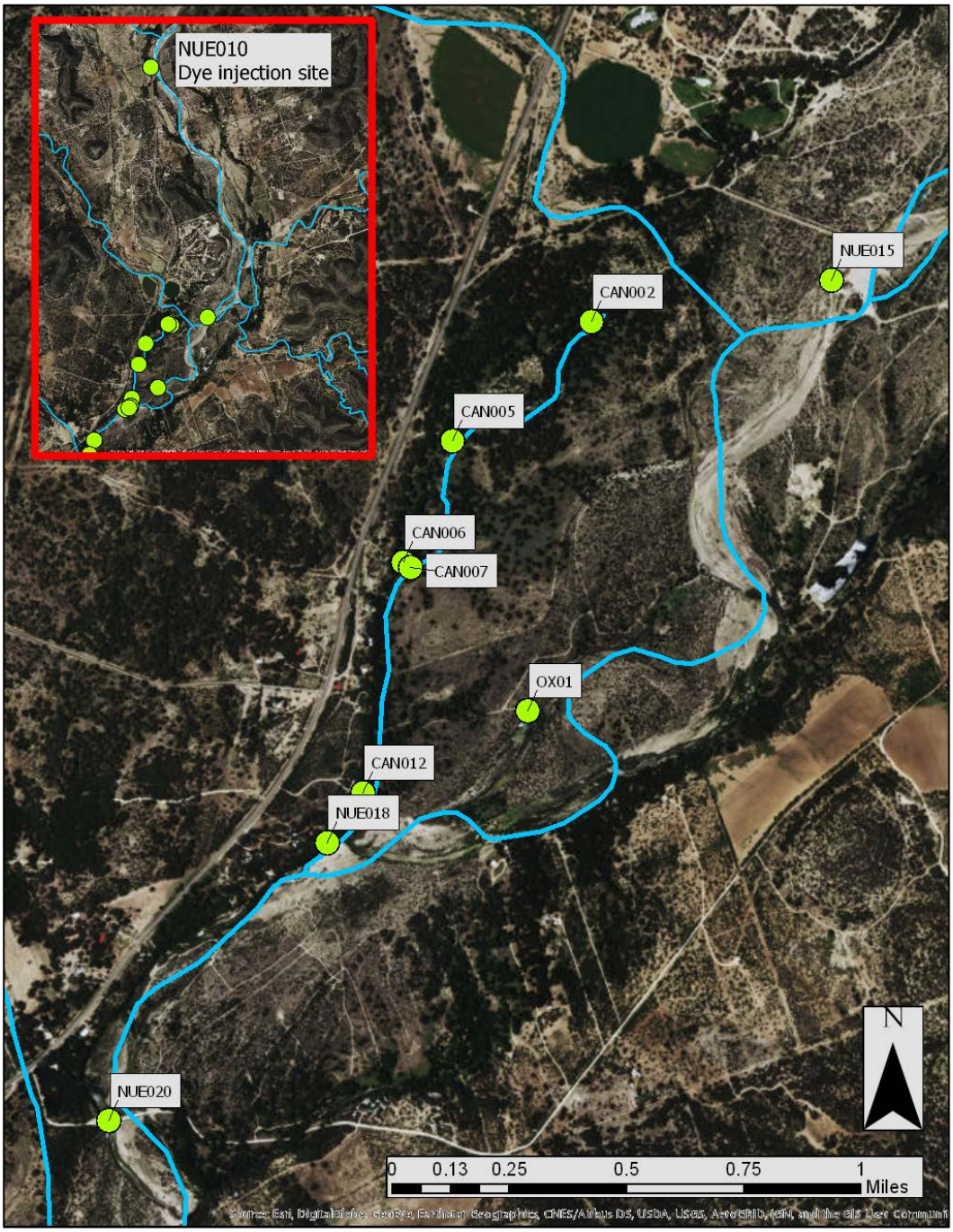

Figure 14. Uranine dye was injected at site NUE010 and monitored at sites along Candelaria Creek, an oxbow pond, and the Nueces River. Streams are approximate and include ephemeral and perennial streams.

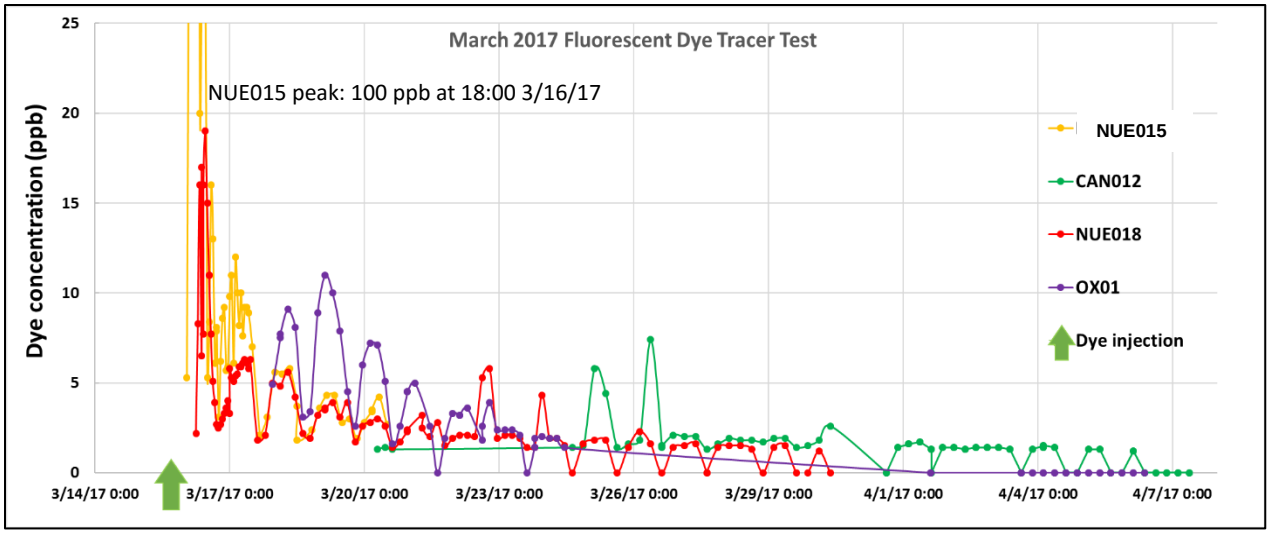

Figure 15. Uranine dye concentration breakthrough curves at selected sites show dye arrival time, peak dye concentration, duration of detectable dye presence, and dispersion effects during transport. Daily variations in dye presence are due to photo-degradation of the dye in sunlight.

Sample site OX01 is the 300m by 20m oxbow pond on an abandoned river channel between Candelaria Creek and the Nueces River. The dye test revealed that the oxbow pond is still in hydrologic communication with the river. The autosampler at site OX01 ran continuously from 03/15/2017 to 03/24/2017, when it became inoperable. It was reset on 04/01/2017 and collected samples through 04/06/2017. The first sample containing uranine was collected on 03/17/2017 at 19:00. The peak concentration was 11.0 ppb on 03/19/2017 at 03:00, four days after dye injection. Decrease in concentration occurred more gradually on the oxbow pond than on the main channel. Uranine remained detectable at OX01 through 03/22/2017, but was undetectable after the autosampler resumed collection on 04/01/2017.

Dye breakthrough occurred in Candelaria Creek at site CAN012 on 03/20/2017, five days after dye injection. It is possible that a peak in concentration occurred during the four day lapse in sample collection (03/21/2017 and 03/25/2017), as the maximum uranine concentration collected was only 7.40 ppb on 03/26/2017. Water samples had detectable fluorescence eight days longer than in the main river channel (NUE018). This is a possible indicator of the slower subsurface flowpaths the dye travels between the Nueces River and Candelaria Creek.

Grab samples and charcoal receptors were used to sample the upstream reaches of Candelaria Creek (CAN002, CAN005, CAN006, and CAN007). Grab samples from CAN002 and CAN005 on 04/01/2017 had 1.5 and 1.4 pb uranine dye, respectively. Charcoal receptors placed on 03/17/2017 at CAN002, CAN005, CAN006, and CAN007 and collected on 04/01/2017 were all positive for dye. The Headwater Spring and Middle Spring had higher concentrations than those in the main stream body, as expected for springs sourced from river underflow. Charcoal receptors placed on 04/01/17 and collected two weeks later on 04/14/17 were still positive for dye at all Candelaria Creek sites. Concentrations were all less than half of what they were in the previous charcoal receptor period (03/17/2017 – 04/01/2017).

Dye traveled down the main channel of the Nueces River at an average speed of 0.2 m/s. Table 6 compares the calculated mean dye velocity between dye detection sites on the Nueces River with the measured stream velocity at the same sites. Dye propagated down the channel much more slowly than the river velocity, likely due to hyporheic

exchange with the subsurface, dye entrapment in eddies and side channels, and dye adsorption to channel bed sediments.

Table 6. Comparison of measured stream velocities and calculated dye velocity in the channel. Dye propagated downstream more slowly than the flow velocity.

River Reach	Measured Mean Stream Velocity (m/s)	Calculated Mean Dye Velocity in Channel (m/s)
NUE010	0.53	n/a
NUE015	0.72	0.213
NUE018	0.36	0.195

Uranine dye was detected at all sampling sites on Candelaria Creek, from the Headwater Spring to CAN012, just upstream of the confluence with the Nueces River. Dye detected at CAN002 and CAN007 confirms that Headwater Spring and Middle Spring are at least partially sourced by the Nueces River under wet conditions. (The CAN007 sampling site is located within the Middle Spring and is separate from the main creek body and therefore not influenced by dye from CAN002.) Dye detected at CAN012 could have resulted from dye entering the creek at the South Springs or from dye traveling downstream from the other two springs. River water could arrive in the creek via diffuse inflow from the shallow alluvium terrace between the creek and the river. A potentiometric map derived from surface water elevations from LiDAR collected in 2014 (Figure 12) confirms that a hydraulic gradient can, at least on occasion, exist that could drive river water to the creek as subsurface flow through alluvium. River water may also

flow through an unmapped karst feature or fault in the bedrock. The subsurface connection with the river could be due to transport in the older alluvial terrace northwest of the Headwater Spring (location of sites LW1 and CW1). This possibility was explored in the second tracer test.

Based on the topography of the study area, it is likely that the dye was transported down the river channel for some distance before it entered the subsurface and subsequently was transported to Candelaria Creek. Four highly simplified, theoretical dye flowpaths are proposed to put first-order constraints on the maximum velocity of dye through the study area (Figure 16). Autosampler data are only available at CAN012; other Candelaria sites were sampled with charcoal receptors and grab samples. Thus CAN012 is the only site with a definitive breakthrough time for the earliest appearance of dye, and the theoretical flowpaths were calculated for various routes from NUE010 to CAN012 based on initial breakthrough time.

Path 1 (Figure 16) assumes that the dye was entirely transported through the subsurface over the total flowpath; this path results in the fastest velocity of dye through the subsurface, 1340 m/day (Table 7). The subsurface is assumed to be homogenous and isotropic over the entire linear path. This path results in an upper limit on dye velocity through the subsurface. Path 1 is not representative of an actual subsurface flowpath through the alluvial deposits, as it crosses limestone hills adjacent to the Nueces that would not transmit flow along the same hypothesized straight-line paths as through the idealized

gravels. Path 1 could be conceptualized as an extended karst conduit flowpath, although this is very unlikely in the Upper Glen Rose.

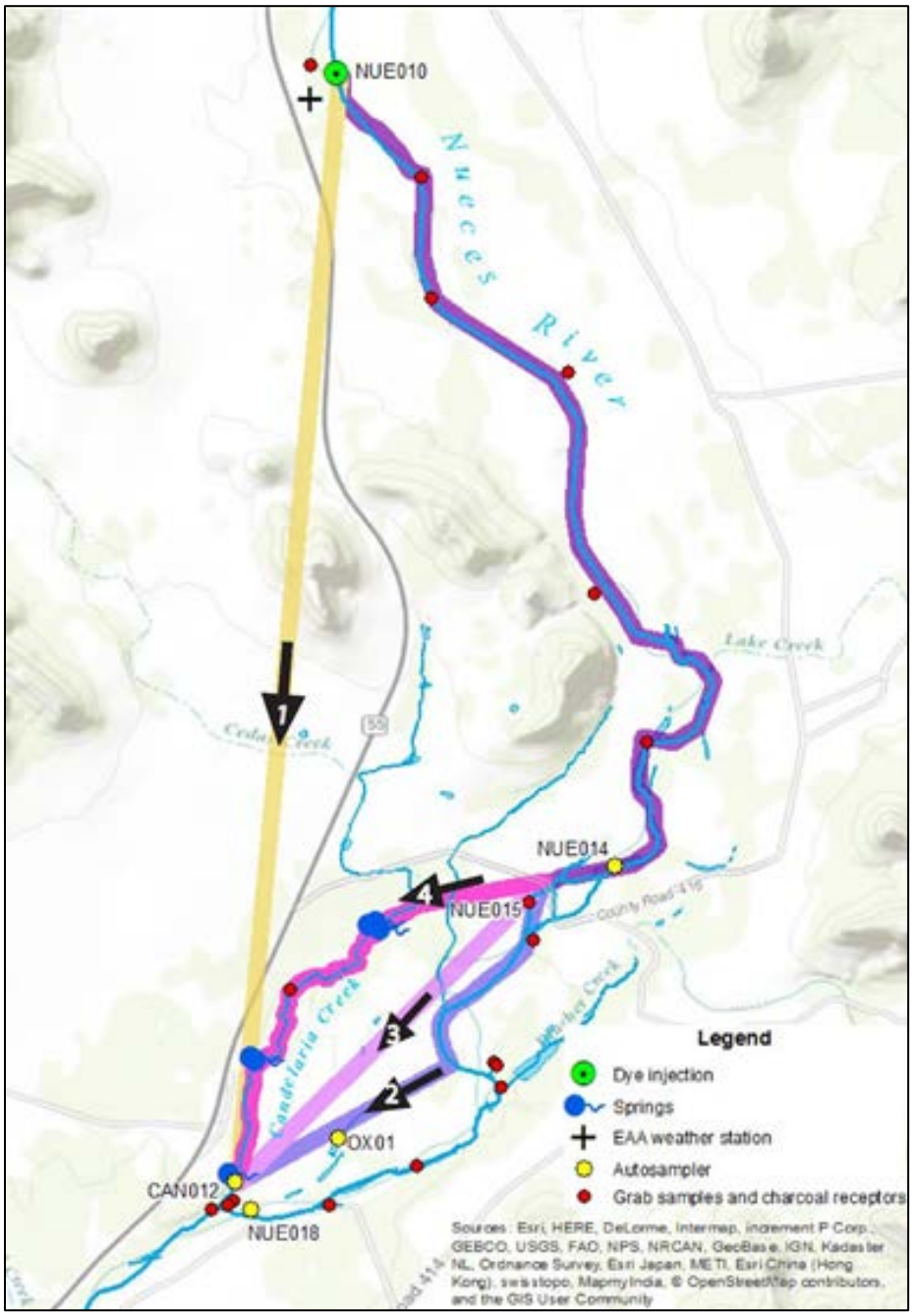

Figure 16. Hypothetical flowpaths from the dye injection point (NUE010) to CAN012 near the terminus of Candelaria Creek.

Paths 2, 3, and 4 involve transport down the river for some distance before the dye enters the subsurface and is transported to Candelaria Creek. These three possible paths are more likely to approximate the way in which dye enters the creek according to the conceptualization of the upper basin as a floodplain conveyance system. In Path 2, dye advects from NUE010 downstream until it is even with the location of an abandoned channel meander on which OX01 is located (oxbow pond). Dye was detected at OX01, confirming a hydraulic connection between the river and oxbow pool. Therefore on Path 2 dye is theorized to flow through the subsurface in a direct path to CAN012 that overlaps with the abandoned meander channel. Calculated dye velocity through the subsurface portion of Path 2 is 527 m/day (Table 7). Similarly, in Path 3 dye advects downstream to NUE015 then moves through the subsurface in a straight path to CAN012 from NUE015. Calculated dye velocity through the subsurface portion of Path 3 is 305 m/day. This calculated dye velocity is faster than on Path 2 because the subsurface path is almost 200 m longer. On Path 4, dye moves down the river to NUE015 then follows a straight path through the subsurface to CAN002 at the headwaters of Candelaria Creek before flowing down the creek to CAN012. Dye was detected with charcoal receptors and grab samples at CAN002, but there is no definitive breakthrough time for dye at CAN002; therefore dye velocity could not be determined. However, subsurface dye velocity on Path 4 is the slowest of all paths because it has the shortest subsurface distance.

The four paths in Figure 16 are simplified approximations of actual flowpaths, but they constrain a range of reasonable dye velocities in the subsurface between the river and

Candelaria Creek. The resulting calculated subsurface velocities and hydraulic conductivities listed in Table 7 are reasonable for well-sorted, coarse alluvial deposits. The higher velocities could be realistic for clast-supported preferential flow paths within gravel bars and terraces.

Table 7. Subsurface flow velocity and hydraulic conductivity of alluvium on four potential flowpaths between the Nueces River and Candelaria Creek.

Path # and Description	**Subsurface flowpath length (m)**	**Apparent subsurface velocity (m/day) (v_{avg})**	**Hydraulic gradient ($\Delta h/\Delta L$) of subsurface path**	**K (m/s) with Φ_{eff} = 0.23**	**K (m/s) with Φ_{eff} = 0.40**
1: Straight subsurface path from NUE010 to CAN012	6,142	801	0.0016	1.31	2.28
2: Along river from NUE010 to abandoned oxbow; straight subsurface path to CAN012	1,266	190	0.0039	1.28E-01	2.22E-01
3: Along river from NUE010 to NUE015; straight subsurface path to CAN012	2,239	314	0.0022	3.75E-01	6.51E-01
4: Along river from NUE010 to NUE015; straight subsurface path to CAN002; along Candelaria Creek to CAN012	821	124	0.0061	5.42E-02	9.42E-02

TESTING ALLUVIAL TERRACE FLOWPATHS

The second fluorescent dye tracer test investigated subsurface flowpaths under low-flow summer conditions to test the assumption that both the alluvial aquifer and river underflow (discharge losses) are sources of springflow in Candelaria Creek. Fluorescent dyes were injected into two irrigation wells located on the alluvial terrace north of the creek headwaters (Figure 17). The LW1 injection well is located within the alluvial Cedar Creek watershed, an ephemeral tributary that flows after heavy rains (anecdotal evidence from landowner). If dye from the LW1 well appeared in Candelaria Creek, it would suggest that Candelaria Creek could be considered an extension of Cedar Creek, despite no surface channel currently connecting them. Close examination of topography using LiDAR suggests that Cedar Creek and Candelaria Creek were once a continuous channel. It was hypothesized that at least the Headwater Spring, and possibly others along the creek, are sourced from alluvial groundwater draining the Cedar Creek watershed to the northwest. Alternatively, the alluvial supply to the Headwater Spring could come from the terrace north of Candelaria Creek. The CW1 injection well is a high-capacity irrigation well (reportedly up to 750 gpm or 0.05 m^3/s) in this terrace, and it was hypothesized that subsurface flow there is connected to the Headwater Spring (CAN002).

There was <0.5 inch (<1.3 cm) precipitation in the study area in the four weeks preceding the test. The Nueces River had zero flow downstream of site NUE015 on the date of the dye injection, and input from Candelaria Creek (23.2 cfs or 0.7 m^3/s) restored the river flow to 23.4 cfs at NUE020. Groundwater levels on the test date show a slight hydraulic gradient between site CW1 (phloxine B injection site) and LW1 (eosin injection

site), suggesting groundwater flow was to the southwest and away from the river (Figure 17). (*N.B.* Figure 17 is a computer-generated potentiometric surface that is used only to show the general trend of the hydraulic gradient.) It is surmised that groundwater pumping from LW1 or LW2 for irrigation use resulted in local drawdown near LW1 and LW2. However it is possible that the hydraulic gradient was not the result of pumping, which suggests that this reach of the upper Nueces River is losing under dry watershed conditions. The subsurface gradient from north to south was 0.003 [unitless] between LW1 and NUE020, suggesting that dye injected in the alluvial terrace would appear in Candelaria Creek or the Nueces River.

Eosin dye injected into well LW1 appeared at monitoring well LW2 eleven hours after injection and peaked 23 hours after injection. Eosin was no longer detectable at LW2 on 08/17/2017, three days after injection. Calculated subsurface velocity based on initial dye breakthrough at LW2 is 5.83E-04 m/s and is 2.79E-04 m/s as calculated with peak concentration time (Table 8). LW2 was pumped at a rate of approximately 2 gpm (1E-04 m^3/s) during the initial monitoring period, which is likely to have slightly increased the observed groundwater velocity.

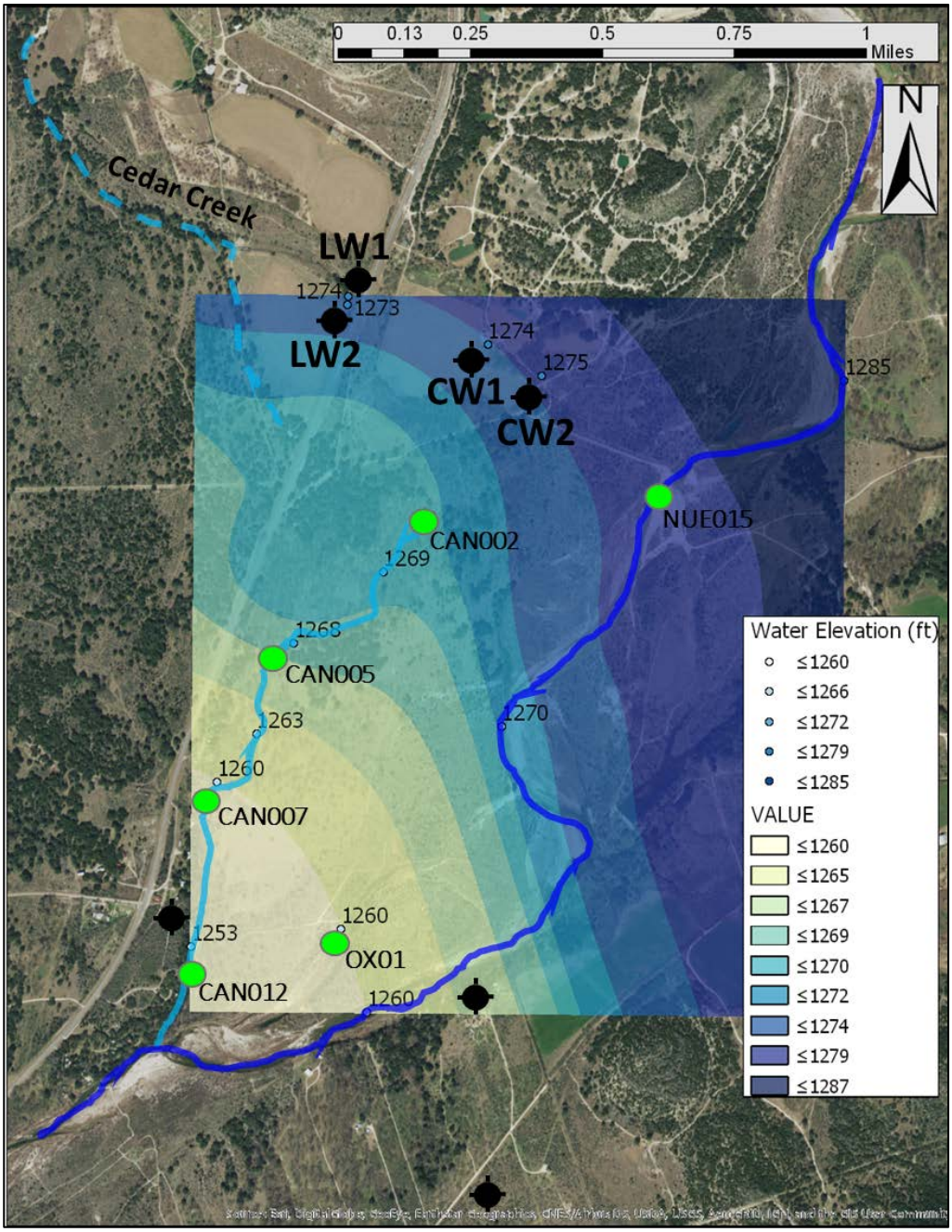

Figure 17. The approximate potentiometric surface within the study area at the beginning of the second fluorescent tracer test (08/14/2017) reveals a gradient from the phloxine B injection site (CW1) and eosin injection site (LW1) towards Candelaria Creek. Wells are marked as black circles; the three unlabeled wells did not test positively for dye. Surface water monitoring sites are marked in green, with an additional site at NUE020.

Table 8. Subsurface flow velocity and hydraulic conductivity of alluvium between the eosin injection well (LW1) and eosin monitoring well (LW2), both located within the alluvial Cedar Creek watershed, northwest of Candelaria Creek.

Path description	Subsurface flowpath length (m)	Apparent subsurface velocity (m/day) (v_{avg})	Hydraulic gradient ($\Delta h/\Delta L$) of subsurface path	K (m/s) with Φ_{eff} = 0.23	K (m/s) with Φ_{eff} = 0.40
Straight path between eosin injection well and eosin monitoring well	25	24.1	0.0048	1.34E-02	2.33E-02

Eosin was detected only at site LW2. Phloxine B dye was not recovered at any monitoring site, including the monitoring well (CW2) located only 200 m away. Sample sites on Candelaria Creek, the Nueces River, and three domestic supply wells were negative for dye during sampling from 08/14/2017—11/05/2017, nearly three months after dye injection. The three domestic supply wells (Figure 17) also tested negative for any background dye from the first tracer test five months earlier. When the landowner restarted pumping from the CW1 well two weeks after dye injection, dye was visible in the well water. The immobility of phloxine B dye at CW1 reflects the heterogeneity of the alluvial terrace and suggests the water table surface is more complex than is mapped in Figure 17.

Only two significant precipitation events occurred in the upper basin between the second dye injection and the final collection of charcoal packets on 11/05/2017 (rain occurred on 09/27/2017 and 10/09/2017). River discharge increased from 12 cfs to 58 cfs

(0.3 m^3/s to 1.6 m^3/s) due to precipitation. Such a change in hydrologic conditions might be expected to flush dye out of storage, yet dye was not detected at monitoring sites after the rain events. This could suggest that in dry conditions, river discharge is stored in alluvium only briefly before entering the Upper Glen Rose Limestone through karst features. Perhaps more likely, gradients within near-channel deposits may have transported the eosin dye into the Nueces River at a point downstream of the monitored sites along a preferential flow pathway within the alluvial terrace. Alternatively, despite the high production rates of the wells and the rapid transmission of eosin between LW1 and LW2, the subsurface flowpaths in the terrace could be disconnected from Candelaria and the river due to lenses of low-conductivity materials such as clay or caliche, which are present in some alluvial wells in the area.

DISAPPEARING DYE: LOSS OF NUECES RIVER—CANDELARIA CREEK CONNECTION IN DRY CONDITIONS

The second dye tracer test revealed different hydrologic behavior during wet and dry floodplain conditions. In August 2017, the Nueces was completely dry downstream of NUE015 before regaining some flow at NUE018 and then receiving inflow from Candelaria Creek. Uranine dye injected at NUE010 was detected only as far downstream as site NUE015 during the second tracer test. Charcoal packets at NUE020 did not test positively for dye during the three-month monitoring period. Nor did uranine dye appear at monitoring sites on Candelaria Creek over the time of observation. In comparison, under relatively wet springtime flow conditions, uranine dye appeared at the downstream end of

Candelaria Creek five days after injection. In the first test, uranine was detected at NUE020 and was visible in the river for several miles downstream of the study area.

It is possible that the discharge lost from the Nueces River between NUE010 and NUE018 in the dry summer months may be held in near-channel deposits with insufficient hydraulic gradient to transport the water to the springs on Candelaria Creek. The floodplain conveyance system could thus be slowed significantly. The river discharge losses may become recharge to the Upper Glen Rose via discrete infiltration into unmapped karst features underlying the alluvium. Candelaria Creek discharge remained relatively high at 23.2 cfs (0.66 m^3/s) on 08/14/2017, suggesting that in dry conditions the springs are sourced from the alluvial aquifer or from slowly-draining, older groundwater in storage in the near-channel, recent deposits.

Baseflow Recession Analysis: Insights into Floodplain Storage

Hydrographs at the three gage locations— NUE010, NUE020, and CAN012— reflect distinct basin storage behavior at each site (Figure 18). Large precipitation events result in flooding at the two river sites, although the timing, magnitude, and duration of the flood stage varies between the upstream and downstream sites. During the relatively dry years of 2013 and 2014, discharge at NUE010 is roughly half of average discharge during wet years. However, the river went completely dry (or was below the measurement threshold) at NUE020 for most of that period. The hydrograph at CAN012 is greatly muted in comparison to the river sites, due to the creek's much smaller drainage area and high

proportion of baseflow. The flood recession on Candelaria rapidly returns to baseflow, suggesting that the river underflow contribution to Candelaria is not greatly affected by flood stages on the Nueces River. Further tracer testing during and after a precipitation event could help determine the relative contribution of river underflow in such conditions. Despite the dry basin conditions of 2013 and 2014, Candelaria Creek discharge never decreased below 6 cfs (0.2 m^3/s). (However these inflows to the river were lost from the channel before they reached the NUE020 gage site.)

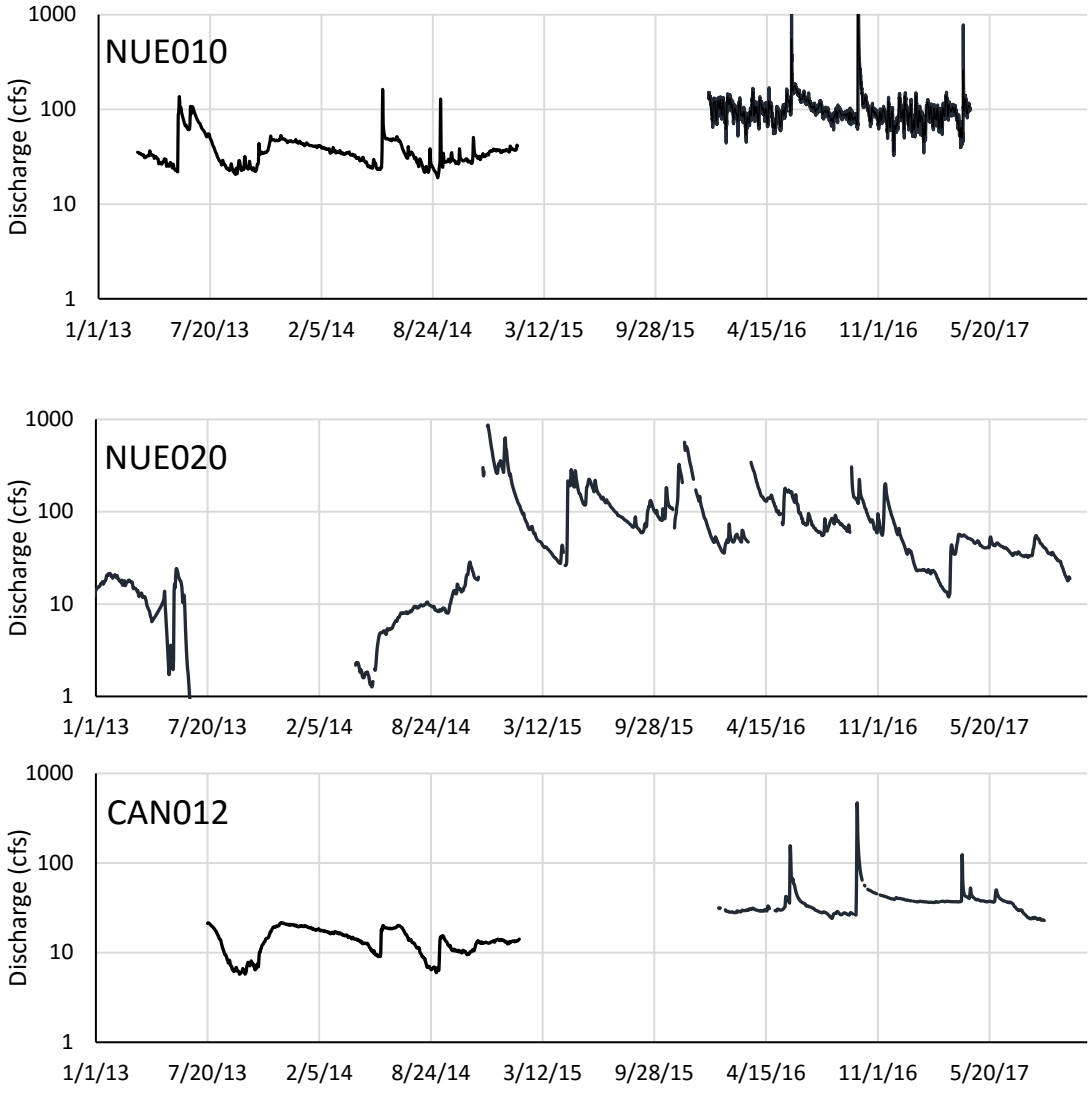

Figure 18. Hydrographs from two sites on the Nueces River and the terminus of Candelaria Creek for the period of 2013—2017.

Summer baseflow following the last precipitation event each spring is plotted in Figure 19 for each gage site. The recession index, *K*, at NUE020 is twice as large as that of NUE010 (Table 9). River discharge diminishes more rapidly at NUE020, suggesting higher losses to alluvial storage or discrete recharge near this site. Interestingly, at NUE020 there is a discharge threshold of roughly 10 cfs (0.3 m^3/s) below which the recession

deviates from linear and decreases more rapidly. This may be due to rapid drainage to karst features when the river stage drops below a certain threshold. In summer 2012, there is an intermediate-sized rainfall event about 50 days after the start of the summer baseflow recession; however, the summer recession rate remained the same following the event despite the new input to the system.

Winter baseflow following the last major storm event of the fall season is plotted in Figure 20. The winter recession is an order of magnitude slower than the summer recession at NUE010 and CAN012, and five times slower at NUE020. This is likely due to a decrease in evaporation due to colder temperatures and a decrease in transpiration during the dormant season. The diurnal discharge fluctuations in the upper basin, as first discussed by Gary and Kromann (2013), are noticeable in Figure 19 and Figure 20. The diurnal fluctuations are larger in the summer season, as expected due to the higher evaporation and transpiration rates.

The recession constant of the Candelaria Creek hydrograph is about an order of magnitude smaller than the river recession constants (Table 9). The streamflow recession on Candelaria is relatively flat, especially during the winter season (Figure 20). Baseflow magnitude varies by year according to the hydrologic condition of the watershed, but the seasonally constant rate suggests that the majority of springflow is supplied by the larger floodplain alluvial aquifer to the north and west of the creek. Baseflow was lower in 2014 than in 2013, suggesting that the alluvial aquifer level had decreased due to the dry 2013 year.

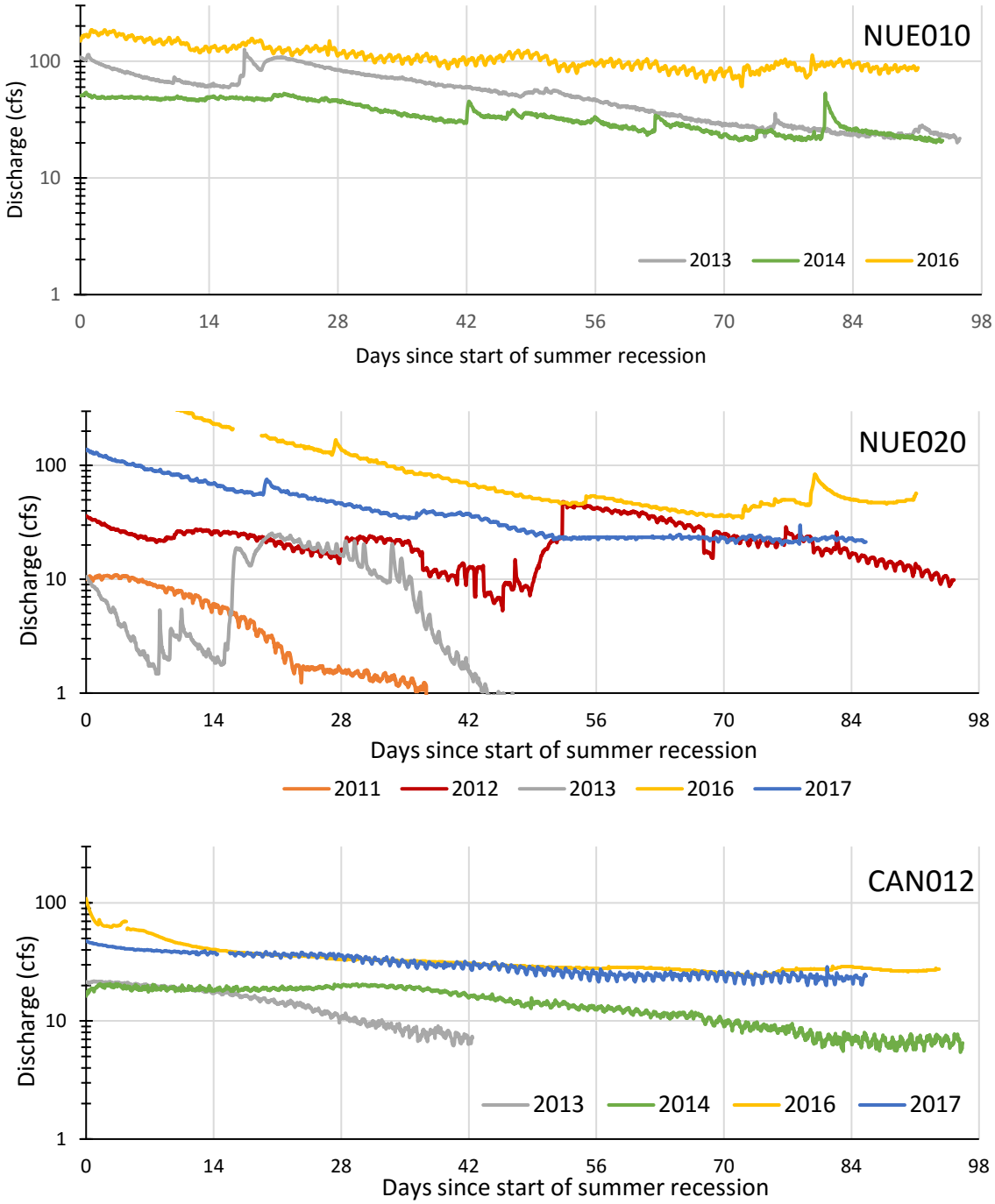

Figure 19. Summer baseflow recession at NUE010, NUE020, and CAN012. Summer baseflow recessions begin annually T* days after the peak discharge of the last major event in the month of May or June.

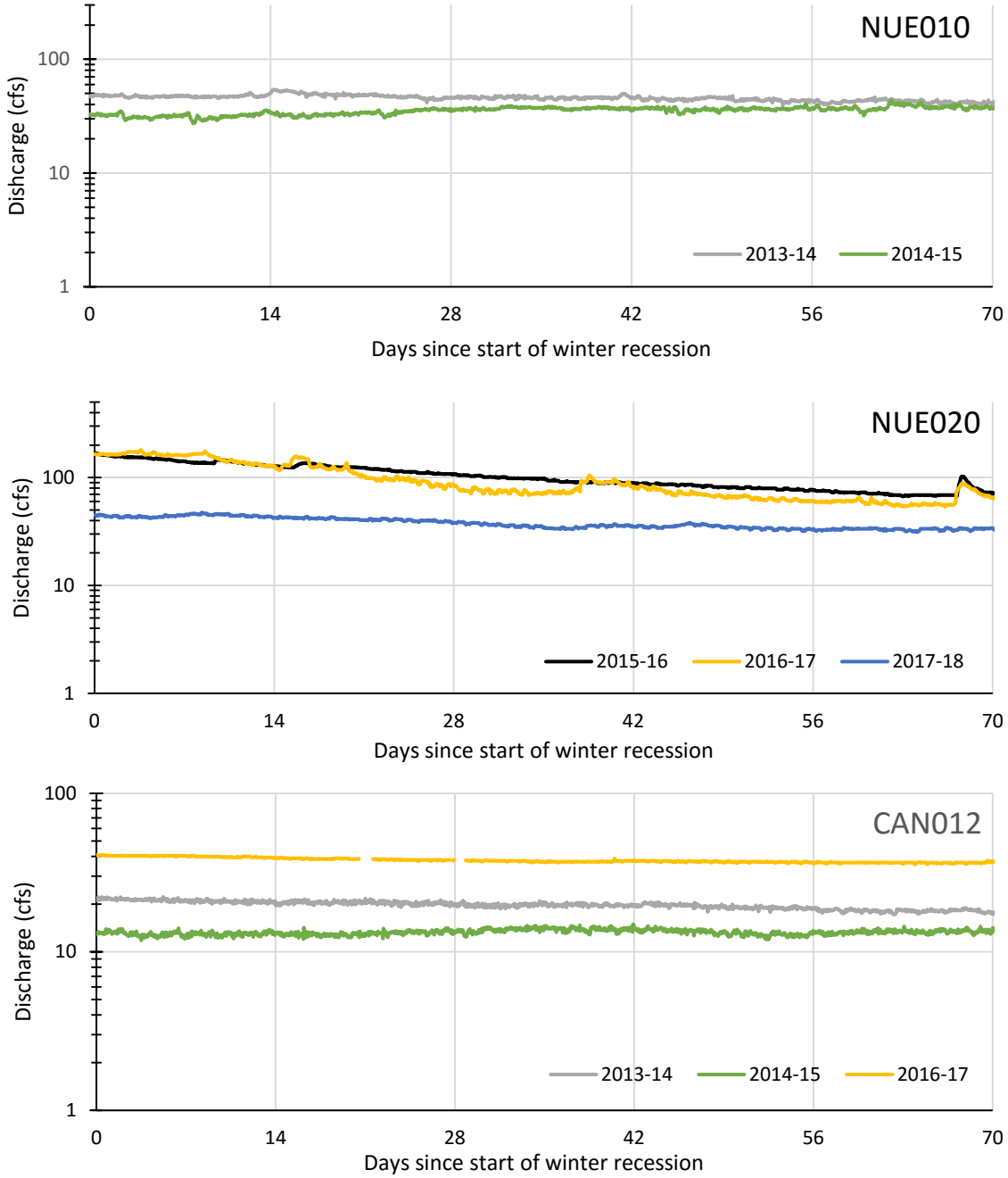

Figure 20. Winter baseflow recession at NUE010 (river upstream), NUE020 (river downstream), and CAN012 (Candelaria Creek). Winter baseflow recessions begin annually T* days after the peak discharge of the last major event in the month of November or December.

Table 9. Baseflow recession constants at sites NUE010, NUE020, and CAN012 for summer and winter seasons. The recession constant, *K*, is unitless and is equal to the slope of the recession curve.

	Recession Constant	
Site	**Average, Summer**	**Average, Winter**
NUE010	0.0338	0.0086
NUE020	0.0807	0.0162
CAN012	0.0171	0.0025

To visualize baseflow recession at the river sites in another way, we use the recession extraction method (REM) of Brutsaert and Nieber (1977) and the recession analysis method (RAM) proposed by Aksoy and Wittenberg (2011) to separate baseflow (Figure 21). Over the 2016—2017 time period, the recessions at NUE010 are flatter while site NUE020 has pronounced recessions during the summer and winter dry seasons. The more rapid recession at NUE020 may be due to loss of streamflow to bank storage in the alluvium or recharge to discrete karst features. The estimated floodplain cross-section at NUE020 (Figure 22) reveals the potential for storage in broad alluvial deposits. The hydrograph at CAN012 is composed nearly entirely of baseflow and thus baseflow there is not plotted separately.

Further calculations (Figure 24, discussed later in this report) revealed the significant contribution of the alluvial aquifer to baseflow. However, a portion of baseflow is likely contributed by the Edwards-Trinity (Plateau) Aquifer, since there are only small scale alluvial deposits in the furthest upstream reaches of the basin.

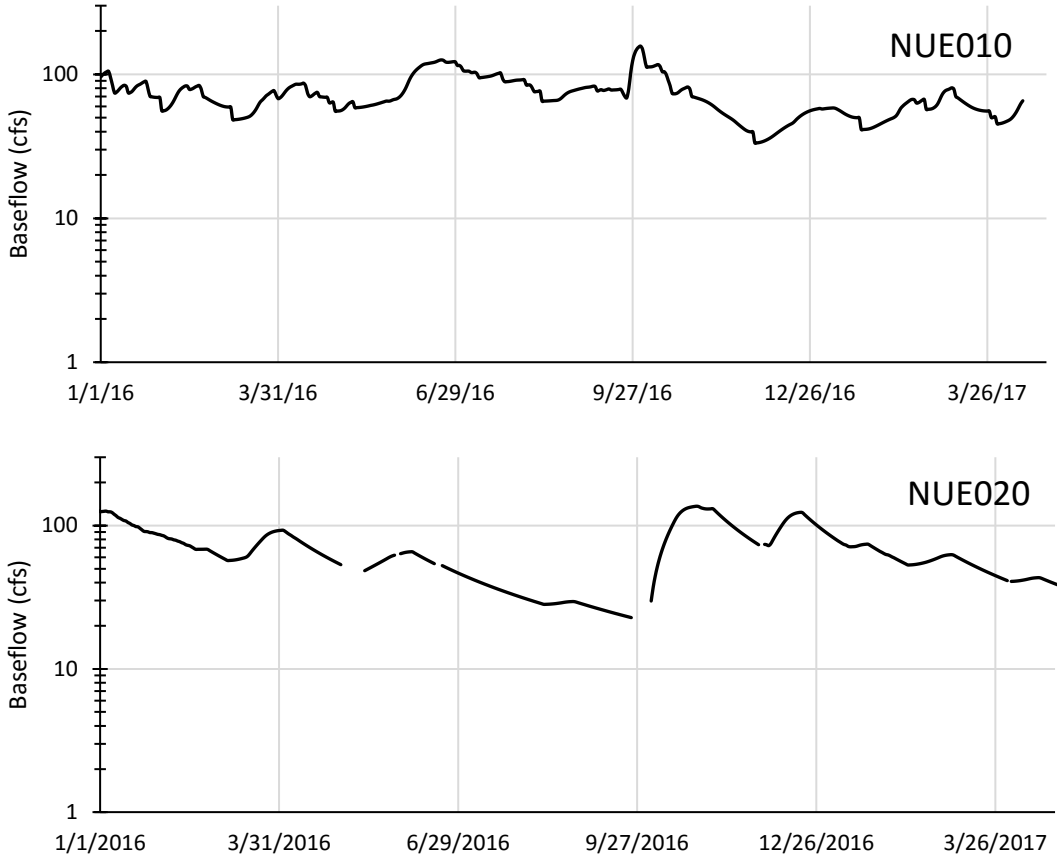

Figure 21. Baseflow (cfs) at sites NUE010 (top) and NUE020 (bottom) from January 2016 – April 2017. Baseflow was separated from total streamflow using the methodology of Brutsaert and Nieber (1977) and Aksoy and Wittenberg (2011).

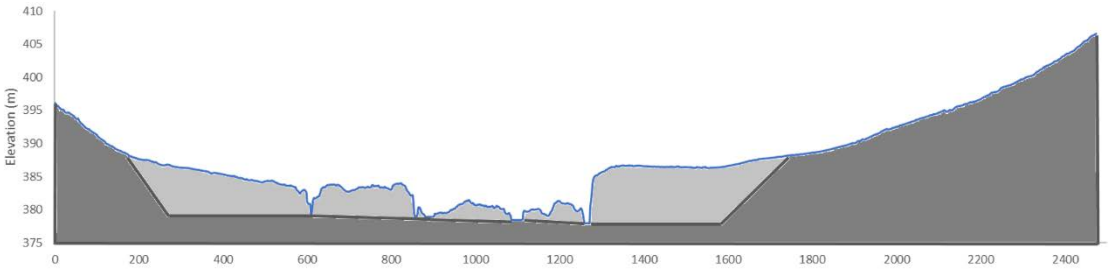

Figure 22. Floodplain cross-section at NUE020 with estimated depth of alluvium based on exposed bedrock in channel beds. Axes are in meters.

Upper Nueces River Basin Alluvial Aquifer Calculations

The intensive local observations around the Candelaria Creek tributary are scaled up to the upper Nueces River watershed to characterize the Nueces River alluvial aquifer. Pumping parameters for several alluvial wells throughout the upper Nueces basin are listed in Table 10. Gravel thickness in the wells varies from 10—29 ft (3—9m), and well yields vary from 6—250 gpm (0.0004—0.02 m^3/s). The Nueces River alluvial aquifer is considered by the Plateau Region Water Planning Group to be a viable aquifer in terms of the state's water planning process (along with the Guadalupe and Frio River alluviums) (LBG-Guyton, 2010).

Table 10. Sample of yields of alluvial wells within the study area. Data is from the TWDB Groundwater Database. Wells are listed by their location from north to south.

Well Tracking Number	Well Yield (GPM)	Drawdown (ft) After One Hour	Gravel Thickness (ft)	Depth to Gravel (ft)
471722	15	0	29	0–29
47507	10	0	18	0–18
402112	15	0	25	27–52
250069	6	25	18	5–23
438375	11	25	17	15–32
38775	15	0	10	20–30
389622	250	7	14	12–26
204687	20	22	18	25–43

Estimations of the total volume of gravel alluvium in the upper Nueces River basin (Figure 5) reveal a significant storage capacity (Table 11). Based on the average gravel layer thickness in the wells, the maximum alluvial groundwater capacity in the upper Nueces basin is 75,480 acre-ft (93.1 x 10^6 m^3). Using the groundwater depths reported in

well logs in the TWDB Groundwater Database, the average alluvial groundwater volume in the upper basin is 21,566 acre-ft (26.6 x 10^6 m^3). This is of course a rough estimate, as the depth-to-water readings were taken at different times and thus under different seasonal hydrologic conditions. Nonetheless, this is an important alluvial groundwater reservoir that contributes baseflow to the Nueces River during low-flow periods. Monitoring wells in the alluvium and alluvial terraces could reveal the degree to which the alluvial aquifer is recharged by the river during high-flow periods.

Within the alluvial outcrop of the upper basin, there are 11 other tributaries with significant alluvial reaches (Figure 23). These tributaries potentially function similarly to Candelaria Creek as part of the floodplain conveyance system that stores water during wet periods and releases baseflow to the river in dry conditions. However, only one of the 11 alluvial tributaries originates within alluvial units as Candelaria Creek does.

Table 11. Groundwater storage capacity in the upper Nueces alluvial aquifer. Based on the methodology of LBG-Guyton Associates (2010).

Parameter	Value
Total area of alluvium outcrop in upper Nueces basin	34,231 acres
Area of productive alluvium outcrop (70%)	23,962 acres
Range in depth to base of gravel in wells	17-35 ft
Mean depth to base of gravel in wells	25 ft
Mean thickness of gravel deposit above bedrock	21 ft
Range in depth to water in wells, from well logs	10-35 ft
Mean depth to water in wells	19 ft
Mean saturated thickness of gravel	6 ft
Maximum groundwater capacity in gravel	**75,480 ac-ft**
Mean volume of groundwater in gravel	**21,566 ac-ft**

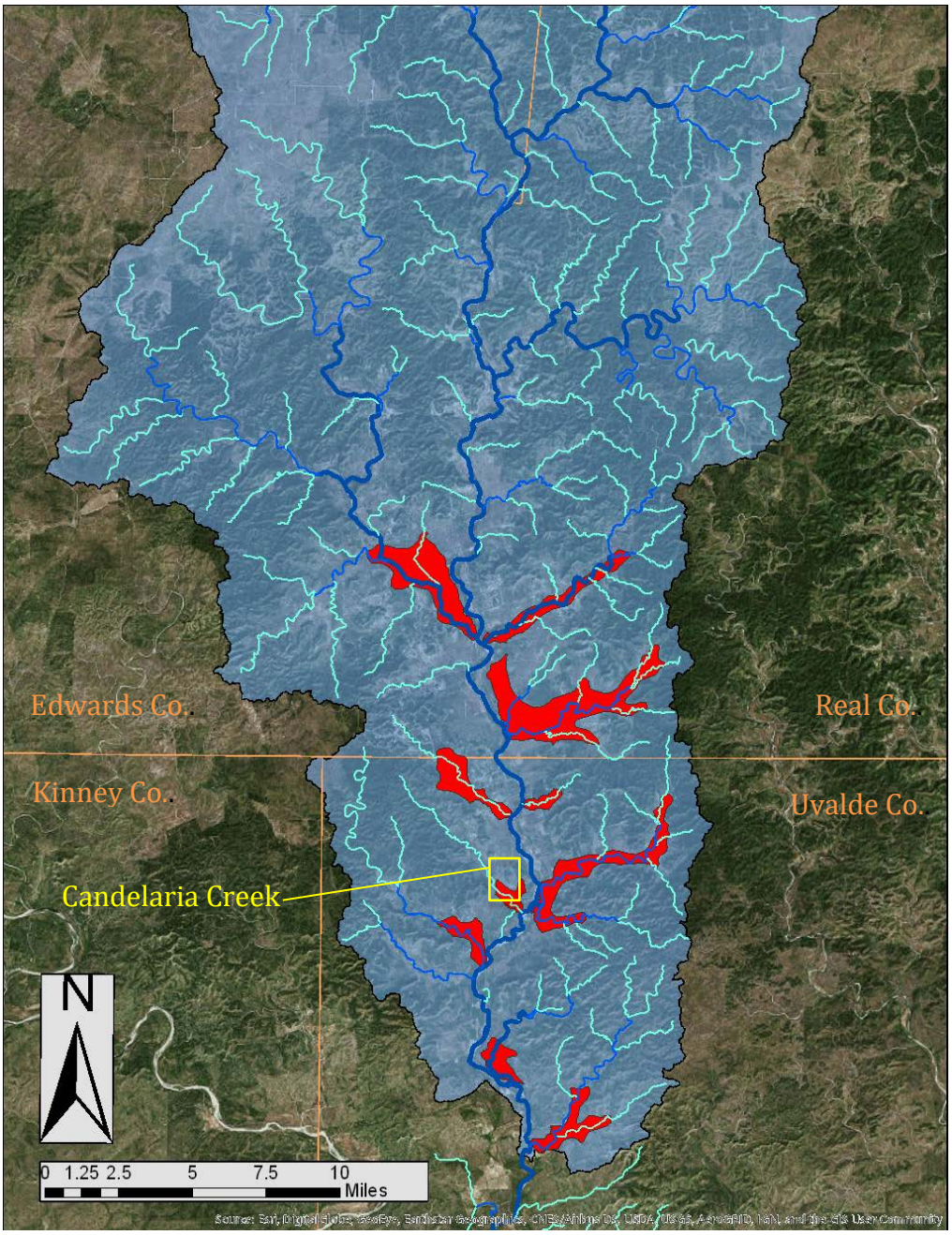

Figure 23. There are 11 other tributaries that drain alluvial units that could behave similarly to Candelaria Creek within the upper basin.

A first-order estimation of the inflow to the Nueces River from the alluvial aquifer reveals the importance of the aquifer during seasonal dry periods and longer droughts (Figure 24). This estimation is based on the conceptualization of the alluvial aquifer as a two-reservoir system: older alluvial terraces with a constant discharge rate and younger, near-river alluvium with a variable discharge that depends on river stage.

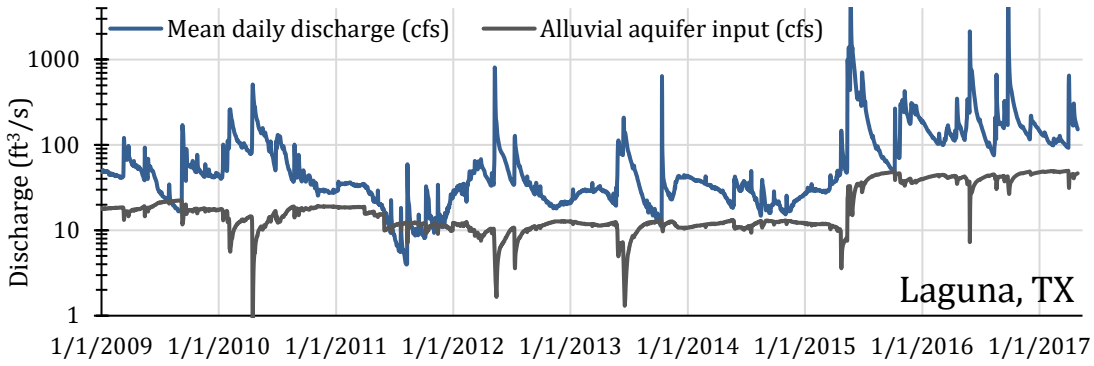

Figure 24. Daily average discharge at the Laguna, TX, gage at the downstream end of the Edwards Aquifer Contributing Zone and estimated alluvial aquifer contribution to river flow.

The contribution of the alluvial aquifer to Nueces River discharge is significant. During the relatively wet basin conditions of May 2015 – April 2017, the alluvial aquifer input into the river was an average of 26% of the measured river discharge at the Laguna gage. The alluvial aquifer contributed an average of 37% of the river discharge during the intermediate watershed condition (January 2009 – May 2011) and 46% of the river discharge during the drought period of May 2011 – May 2015. During low flows, the alluvial aquifer accounts for 100% of river discharge on some occasions. This simple

estimation also overestimates the river discharge over three periods, when the decrease in the measured river discharge outpaces the decrease in the measured gage height. During flood events, the gradient within the near-river alluvial reservoir is reversed, resulting in the sharp decreases in alluvial aquifer input seen in Figure 24.

4. DISCUSSION

Candelaria Creek Spring Sources

UPDATED CONCEPTUAL MODEL OF THE UPPER NUECES RIVER BASIN

Researchers at least as far back as Brune (1981) have hypothesized that the springs around Montell, TX, are sourced from river underflow that "intermittently sinks into gravel beds and reappears as springs" (Brune, p. 41). In a 2015 study of Candelaria Creek springflow, Kromann used specific conductance, temperature, chemical and isotopic data, and a basin water balance to conclude that 80% of Candelaria springflow is sourced from the Nueces River and 20% is from groundwater. In her conceptual model of the basin, Kromann assumed that the groundwater contribution was sourced from the Trinity Aquifer, as she did not differentiate between alluvial- and carbonate-sourced groundwater. In her study of the impact of *Arundo donax* (giant cane), Jain (2014) adapted the Soil Water Assessment Tool (SWAT) for the upper Nueces River basin. The SWAT model is based on five linear reservoirs, including ones for the subsurface and surface runoff (Arnold et al., 2012). Jain (2014) partitioned the subsurface into shallow and deep karst aquifers and made adjustments at the subbasin level to account for variability in baseflow recession and

recharge due to karst features. She adjusted model parameters that govern baseflow recession, the time delay of recharge, and the partitioning of shallow recharge and deep recharge. However, Jain did not explicitly recognize or address the alluvial aquifer or non-karst groundwater flow.

Based on the results of dye tracer tests, hydrologic mass balance, and a review of well logs in the upper Nueces River basin, I conceptualize the floodplain as a mantled alluvial aquifer over the carbonate bedrock of the Edwards-Trinity (Plateau) Aquifer. Although karst flow and discreet recharge certainly occur, especially within the active channel zone, the majority of baseflow to the river channel—and to Candelaria Creek—is sourced from alluvial storage. Candelaria springflow is greater in volume than the discharge lost from the Nueces River, suggesting that the contribution of alluvial groundwater must be larger than the 20% groundwater contribution suggested by Kromann (2015). This is especially true during extended dry periods, when the river underflow component of springflow approaches zero.

Measurements of carbon-14 taken in August 2017 by the Barton Springs/ Edwards Aquifer Conservation District (unpublished) within the study area support this conceptualization of an alluvial floodplain conveyance system (Table 12). The apparent age of river water, Candelaria Headwater Spring, and Candelaria Middle Spring are comparable. Well water at LW1 (eosin injection site), while older than the other samples from the study area, is significantly younger than samples from the Edwards-Trinity (Plateau) Aquifer from nearby Val Verde County (Kreitler et al., 2013).

Table 12. Carbon-14 measurements from shallow water sources within the upper Nueces River floodplain conveyance system are similar, while Edwards-Trinity (Plateau) Aquifer groundwater is significantly older.

Site	Carbon-14, Diss. Apparent Age (Years BP)	Carbon-14 Fraction Modern
Nueces River (NUE020)[1]	170	0.979
Candelaria Headwater Spring (CAN002)[1]	240	0.9711
Candelaria Middle Spring (CAN007)[1]	270	0.9671
Uvalde Gravel Aquifer (LW1)[1]	410	0.95
E-T (Plateau) Aquifer, Val Verde Co.—Shallow wells[2]		0.3-0.74
E-T (Plateau) Aquifer, Val Verde Co.— Deep wells[2]		0.27-0.6

[1] Sample collected on 08/07/2017 for the TWDB Groundwater Database.
[2] Sample collected for the TWDB report by Kreitler et al. (2013, pg. 56).

DYNAMIC ALLUVIAL FLOODPLAIN CONVEYANCE SYSTEM

The relatively rapid transmission of uranine dye through the high conductivity sediments of the near-channel terrace during the first tracer test suggests that the Nueces River and Candelaria Creek have a strong hydraulic connection under wet watershed conditions. Uranine dye appeared in Candelaria Creek five days after dye injection in the first test. The hydraulic connection is lost, or significantly slowed, in dry conditions, as evidenced by the lack of dye found in the creek during the second tracer test. Dye was not detected in Candelaria Creek for three months after the second tracer test, though it may have eventually been driven out of storage in alluvium by an increase in river stage in the spring rainy season. Alternatively, the dye may never have appeared in the creek and rather became recharge to the Edwards-Trinity (Plateau) Aquifer. The hydraulic gradient between the river and creek was 0.003 [unitless] during both tracer tests based on surface water

elevations. It is likely that below a certain river stage, the high conductivity flowpaths between the river and creek are not active. Although it receives no river underflow during dry periods, Candelaria Creek always has a baseflow greater than 6 cfs (0.2 m^3/s) (this minimum flow occurred in September 2013 and September 2014), which confirms the input of alluvial terrace groundwater. The second dye tracer test revealed that the floodplain alluvial aquifer has significant hydraulic conductivity even in the summer, as observed between wells LW1 and LW2.

Inter-seasonal variability in the baseflow recession rate is common in many watersheds due to fluctuations in evapotranspiration and antecedent aquifer storage (Bart, 2014). These fluxes from the aquifer increase, or steepen, the recession rate, which is evident when comparing the summer and winter baseflow recession indices (Figure 19, Figure 20, and Table 9). Land cover in the upper Nueces River basin is a mix of shrub land and forest. The alluvial terrace around Candelaria Creek is densely forested with mature pecan trees. Anecdotal evidence from landowners suggests that the growing season of pecan trees in particular has an impact on springflow in the upper basin. Pecan trees start budding in March and mature trees require roughly 100—200 gallons (0.4—0.8 m^3) of water per day from April through October (Lipe et al., n.d.). Mr. Bill Luce, who manages land near Candelaria Creek, reported on July 14, 2017 that springflow increases in late October once pecan trees go dormant.

Plots of the Normalized Difference Vegetation Index (NDVI) and the Enhanced Vegetation Index (EVI) for the areas of alluvium outcrop in the upper Nueces basin reflect

the seasonal vegetation cover (Figure 25). These vegetation indices are derived from the National Oceanic and Atmospheric Administration's Advanced Very High Resolution Radiometer (AVHRR) data and measure the density of green vegetation on the Earth's surface. Many studies have found that the indices have a strong linear relationship with evapotranspiration (Alemayehu et al., 2017; Szilagyi et al., 1998; Loukas et al., 2004). The plots in Figure 25 are a composite of the indices for 16 alluvium sites in the study area; they reveal the seasonal dynamics of vegetation cover and are a proxy for rates of evapotranspiration (ET) in the basin. ET is high during the spring and summer growing season and decreases in the winter. The impact of water stress from the 2011 drought is exhibited by the decreased indices in that year.

It is worth noting that the impact of the invasive giant cane species *Arundo donax* on the hydrologic regimes of Texas rivers is of growing concern to landowners and watershed managers. Jain (2014) evaluated its impact in the upper Nueces River riparian zone. In a comparison to the native switchgrass, the accumulated ET and water yield were not statistically different over the study period (1995-2010), suggesting that *A. donax* has not changed the watershed dynamics. Therefore, *A. donax* has likely not affected the exchange of Nueces River underflow with the alluvial aquifer. Gary and Kromann (2013) also studied the impact of *A. donax* on riparian flow in the upper Nueces River. No direct connection was found between *A. donax* transpiration and the daily cyclical fluctuations in observed flow at the USGS gage in Laguna, TX (site 33, Figure 7).

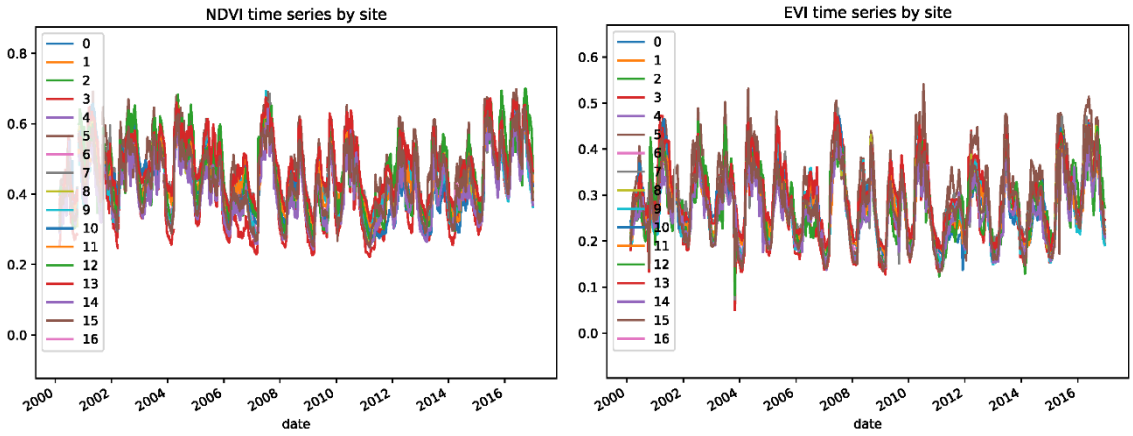

Figure 25. Normalized Difference Vegetation Index (NDVI) and the Enhanced Vegetation Index (EVI) for the areas of alluvium outcrop in the upper Nueces basin (courtesy of Jesse Hahm, unpublished figure).

EVIDENCE FOR PREFERENTIAL FLOWPATHS WITHIN NEAR-CHANNEL DEPOSITS

There are a few probable explanations for the apparent disappearance of dye that was injected into the Nueces River during the second tracer test. Floodplain mass balance calculations indicate ample storage potential in the alluvial deposits within the study area to accommodate the Nueces River discharge losses. The eosin dye injected into the alluvial terrace northwest of Candelaria Creek during the second tracer test may have been transported through the subsurface along a preferential flowpath that bypasses the creek. Preferential flowpaths (PFP) are linear features of high conductivity sediments, such as paleochannels, which can link streamflow with more distant floodplain areas (Miller et al., 2016). The eosin injection and monitoring wells may be sited on a paleochannel of the ephemeral Cedar Creek to the northwest of Candelaria Creek (Figure 17). Alluvial groundwater draining from the Cedar Creek watershed along a paleochannel may have

transported the dye out of the terrace, explaining the apparent disappearance of dye after the second tracer test. The PFP may discharge into the Nueces River in accordance with the general conceptualization of the floodplain gradient, but at a location downstream of the dye monitoring sites.

EVIDENCE FOR DISCRETE DRAINAGE TO UNDERLYING KARST AQUIFER

Another explanation for the unrecovered dye during the second tracer test is drainage from the river and the alluvial aquifer to the underlying karst bedrock. Although the floodplain mass balance calculations within the study area revealed that there is sufficient alluvium storage capacity to transfer all of the river discharge losses from the Nueces River to Candelaria Creek, discrete recharge to karst features and transport in the karst bedrock is certainly still possible. High-density fracture sets are visible in the riverbed at two sites upstream of site NUE010 (Figure 27). These fractures are coincident with regional faulting and fracture sets in the Devils River trend of the Edwards Plateau, and are likely present throughout the study area although obscured by alluvium. Figure 26 is a simplified conceptual model of the fracture sets overlain by the alluvial aquifer. The recharge rate depends on the saturated thickness of alluvium (h_{sat}), hydraulic conductivity of alluvial sediments, secondary porosity of limestone including fracture aperture (Δx), and fracture density.

The installation of a transect of piezometer wells in alluvium could be used to further quantify the drainage flux out of the alluvial aquifer. Because the hydrologic mass balance for the study area revealed that there is enough storage capacity in alluvium to

account for all of the river discharge losses, more data is needed to estimate the portion that becomes bedrock recharge. Water level measurements in the alluvial and carbonate aquifers are needed to produce a first-order estimate of discrete recharge within the study area.

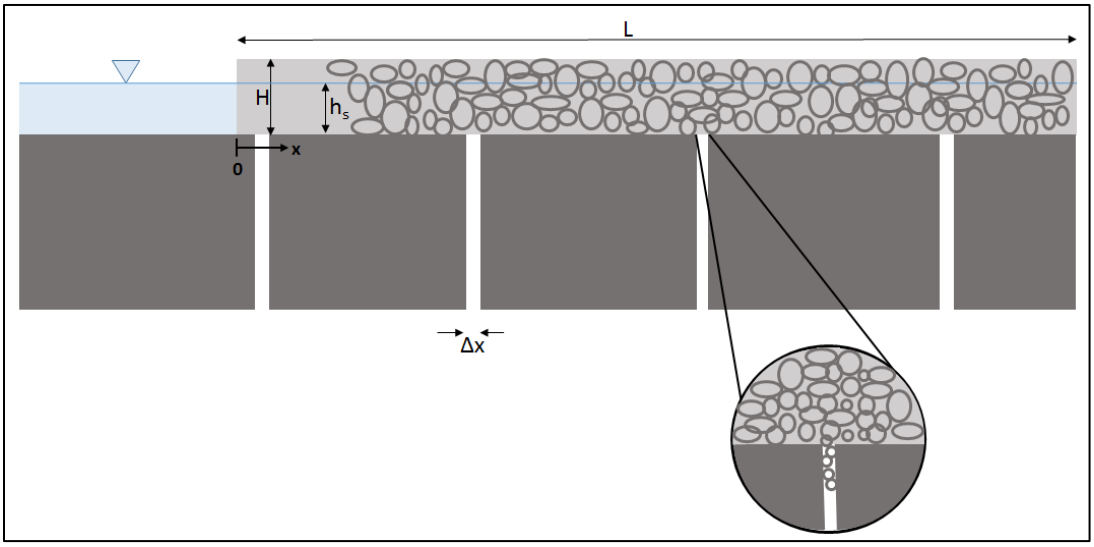

Figure 26. Conceptual diagram of drainage from a gravel deposit of depth, *H*, and width, *L*, into carbonate bedrock fractures of aperture, Δ*x* (not to scale).

Figure 27. Fractures visible in the carbonate bedrock of the Nueces River two miles (3.2 km) upstream of site NUE010, near the Real County – Uvalde County line.

Implications for Edwards Aquifer Recharge

It is critical for managers of the Edwards Aquifer to quantify recharge in order to manage the resource sustainably. A major question of this study is whether streamflow losses within the EACZ of the upper Nueces River basin should be considered recharge to the Edwards Aquifer. The updated conceptual model developed from tracer testing, hydrograph analyses, and groundwater mass balances suggests that the majority of streamflow losses are held in storage in alluvium and gradually released back to the river as baseflow. In this way, the alluvial aquifer impacts the timing and magnitude of recharge throughout the year by providing a more constant river discharge that flows into the EARZ and recharges the Edwards Aquifer. Some discharge losses from the upper Nueces River do become discrete recharge via karst features in the stream channel and under the mantled alluvium; however, the current study did not quantify discrete recharge. Future groundwater level data for the alluvial and carbonate aquifers could make a first-order approximation of discrete recharge possible using a water balance approach.

Figure 24 reflects the integrated effect of the entire alluvial aquifer upstream of the town of Laguna and the EARZ. Without the storage of river underflow in alluvium and the delayed release from storage, discharge at Laguna would be significantly reduced and the river would likely have gone completely dry during the summers of drought years. Flood peaks would likely be greater without the buffering effect of temporary storage in near-channel alluvial deposits.

This approach is based on the conceptualization of the alluvial aquifer as a dynamic two-reservoir system, and it integrated measured river discharge and known or suitable estimates of alluvial aquifer properties. This methodology simplifies the heterogeneity of the alluvial sediments and the geometry of the floodplain. Bedrock 'highs' are likely to produce points of discontinuity within the alluvial area, and lenses of caliche or clay may reduce lateral continuity of the groundwater flux. The method could be improved with measurements of groundwater head in the alluvial terraces and the near-channel alluvium along the longitudinal floodplain axis, as well as field measurements of hydraulic conductivity and storativity.

5. CONCLUSIONS AND FUTURE RECOMMENDATIONS

The goal of this study was to quantify the storage capacity and drainage characteristics of the upper Nueces River alluvial aquifer in order to investigate its effects on streamflow. Intensive field investigations were carried out in a representative river reach around Candelaria Creek, an important spring-fed tributary. Differential gaging revealed significant gains and losses of the Nueces River within the Edwards Aquifer Contributing Zone, which is typically conceptualized as a drainage area, not a recharge area. To investigate whether the measured river discharge losses become Edwards Aquifer recharge or alluvial aquifer recharge, several field and analytic methods were applied. Fluorescent dye was used to trace shallow subsurface pathways along the river and in alluvial terraces,

confirming that the Nueces River and Candelaria Creek are hydraulically connected during the wet season. Floodplain mass balance calculations suggested that the alluvial aquifer within the study area has sufficient capacity to transmit the entirety of the discharge lost from the river in the study reach. Hydrograph analyses revealed variable baseflow recession behavior between the wet and dry seasons. The dye tracer tests proved that the connection between the river and creek can be lost during dry basin conditions.

Near-channel alluvium deposits and alluvial terraces in the upper Nueces River basin comprise a significant aquifer overlying the carbonate bedrock, with an estimated maximum alluvial groundwater capacity of over 75,000 acre-ft (92.5×10^6 m^3). Temporary storage of river underflow within near-channel alluvium and the slow drainage of older groundwater from terraces are important to baseflow in the Nueces River. During the relatively wet basin conditions, the alluvial aquifer in the upper Nueces River basin contributed an average of 26% of the measured river discharge. The alluvial aquifer contribution was on average 37% of river discharge during the intermediate watershed condition and 46% of river discharge under drought condition. During low flows, the alluvial aquifer can account for 100% of river discharge. These contributions extend baseflow during both seasonal summer dry conditions and multi-year drought periods, and therefore increase the recharge from the Nueces River to the Edwards Aquifer downstream in the EARZ.

While this study established that the upper Nueces basin alluvial storage is large, dynamic, and supplies baseflow to the Nueces River for recharge in the EARZ, future work

is needed to further quantify alluvial storage dynamics. Future researchers could install and continuously log alluvial wells to study short-term storage during and after flood events. A transect of wells in alluvium between the river and Candelaria Creek would be ideal. These wells could be used to establish the potentiometric surface in wet and dry basin conditions. An additional transect of wells perpendicular to the river and extending to the older alluvial terraces in the study area would quantify the hydraulic gradient between the broader alluvial aquifer and the near-channel alluvium deposits. Future studies could be used to determine if the 11 other alluvial tributaries in the upper basin function similarly to Candelaria Creek.

REFERENCES

Aksoy, H. and Wittenberg, H., 2011, Nonlinear baseflow recession analysis in watersheds with intermittent streamflow: Hydrologic Sciences Journal, v. 56, p. 226-237.

Alemayehu, T., van Griensven, A., Senay, G.B., and Bauwens, W., 2017, Evapotranspiration mapping in a heterogeneous landscape using remote sensing and global weather datasets: application to the Mara Basin, East Africa: Remote Sensing, v. 9, doi: 10.3390/rs9040390

Anaya, R., Boghici, R., French, L., Jones, I., Petrossian, R., Ridgeway, C., Shi, J., Wade, S., Weinberg, A., 2016, Texas aquifers study, Texas Water Development Board Report.

Arciniega-Esparza, S., Brena-Naranjo, J.A., Pedrozo-Acuna, A., and Appendini, C.M., 2017, Hydrorecession: a Matlab toolbox for streamflow recession analysis: Computers and Geosciences, v. 98, p. 87-92.

Arnold, J. G., Moriasi, D.N., Gassman, P.W., Abbaspour, K.C., White, M.J., Srinivasan, R., Santhi, C., Harmel, R.D., van Griensven, A., Van Liew, M.W., Kannan, N., and M.K. Jha, 2012, SWAT: model use, calibration, and validation: Transactions of the American Society of Agricultural and Biological Engineers, v. 55, p. 1491-1508.

Barnes, V.E. (project director), 1974, Geologic atlas of Texas, Seguin sheet: University of Texas-Austin, Bureau of Economic Geology Geologic Atlas of Texas, scale 1:250,000, Donald Clinton Barton memorial edition.

Barnes, V.E., 1977, Geologic atlas of Texas, Del Rio sheet: University of Texas-Austin, Bureau of Economic Geology Geologic Atlas of Texas, scale 1:250,000, Robert Thomas Hill memorial edition.

Banta, J.R., Lambert, R.B., Slattery, R.N., and Ockerman, D.J., 2012, Streamflow gain and loss and water quality in the upper Nueces River basin, south-central , Texas , 2008 – 10: US Geological Survey Scientific Investigations Report 2012-5181.

Bart, R., and Hope, A., 2014, Inter-seasonal variability in baseflow recession rates: The role of aquifer antecedent storage in central California watersheds: Journal of Hydrology, v. 519, p. 205–213, doi: 10.1016/j.jhydrol.2014.07.020.

Barker, R.A., Bush, P.W., and Baker, E.T., 1994, Geologic history and hydrogeologic setting of the Edwards-Trinity aquifer system, west-central Texas: US Geological Survey Water Resources Investigations Report 94-4039.

Brune, G., 1975, Report 189: Major and historical springs of Texas: Texas Water Development Board, p. 94.

Brune, G., 1981, Springs of Texas: v. 1: Fort Worth: Branch-Smith Inc., 114 p.

Brutsaert, W., and Nieber, J.L., 1977, Regionalized drought flow hydrographs from a mature glaciated plateau: Water Resources Research, v. 13, p. 637–643, doi: 10.1029/WR013i003p00637.

Clark, A.K., 2003, Geologic framework and hydrogeologic characteristics of the Edwards Aquifer, Uvalde County, Texas: US Geological Survey Water-Resources Investigation Report 03-4010.

Dingman, S.L., 2002, Physical hydrology, 2nd ed.: Upper Saddle River, NY, Prentice Hall, 646 p.

Edwards Aquifer Authority, 2017, Hydrologic data report: 2016 recharge, 8 p., https://www.edwardsaquifer.org/files/download/hydro/2016-Recharge-Report.pdf.

Fetter, C. W., 1994, Applied Hydrogeology, 3rd ed.: London, Pearson.

Gary, M. and Kromann, J., 2013, Evaluation of riparian water flux patters in the upper Nueces, Sabinal, Frio, and Dry Frio rivers, Texas in relation to the control of Arundo Donax: Edwards Aquifer Authority Report for Task 3 Arundo Donax Control and Restoration Project II.

George, P.G., Mace, R.E., and Petrossian, R., 2011. Aquifers of Texas, Texas Water Development Board Report 380.

Green, R.T., Bertetti, F.P., Franklin, N.M., Morris, A.P., Ferrill, D.A., and Klar, R. V, 2006, Evaluation of the Edwards Aquifer in Kinney and Uvalde Counties, Texas: Report prepared for the Edwards Aquifer Authority, 113 p.

Green, R.T., Winterle, J.R., and Prikryl, J.D., 2008, Discharge from the Edwards Aquifer through the Leona River floodplain, Uvalde, Texas 1: Journal of the American Water Resources Association, v. 44, p. 887–901.

Gustavson, T.C., 1978, Bed forms and stratification types of modern gravel meander lobes, Nueces River, Texas: Sedimentology, v. 25, p. 401–426, doi: 10.1111/j.1365-3091.1978.tb00319.

Hauwert, N., 2016, Stream recharge water balance for the Barton Springs segment of the Edwards Aquifer: Journal of Contemporary Water Research and Education, v. 159, p. 24-49.

Hauwert, N. and Sharp, J.M., Jr., 2014, Measuring autogenic recharge over a karst aquifer utilizing eddy covariance evapotranspiration: Journal of Water Resource and Protection, v. 6, no. 9.

Heath, R.C., 1983. Basic ground-water hydrology, U.S. Geological Survey Water-Supply Paper 2220, 86p.

Heeren, D.M., Fox, G.A., Fox, A.K., Storm, D.E., Miller, R.B., and Mittelstet, A.R., 2014, Divergence and flow direction as indicators of subsurface heterogeneity and stage-dependent storage in alluvial floodplains: v. 1317, p. 1307–1317, doi: 10.1002/hyp.9674.

Hemphill, L.H., 2005, Hydrogeology of heterogeneous alluvium in the Leona aquifer, Caldwell County, Texas [MS thesis]: University of Texas at Austin, 179 p.

Jain, S.P., 2014, Modeling hydrologic impact of Arundo donax on headwaters of the Nueces River using SWAT model [MS thesis]: Texas A&M University, 98 p.

Keshavarzi, M., Baker, A., Kelly, B.F.J., and Andersen, M.S., 2017, River–groundwater connectivity in a karst system, Wellington, New South Wales, Australia: Hydrogeology Journal, v. 25, p. 557–574, doi: 10.1007/s10040-016-1491-y.

Kreitler, C. W., Beach, J. A., Symank, L., Uliana, M., Bassett, R., Ewing, J. E., and Kelley, V. A., 2013, Evaluation of hydrochemical and isotopic data in groundwater management areas 3 and 7, Texas Water Development Board.

Kromann, J., 2015, Surface water recharge in karst: Edwards-Trinity Aquifers-Nueces River system [MS thesis]: University of Texas at Austin, 209 p.

Larkin, T.J. and Bomar, G.W., 1983, Climatic atlas of Texas: Texas Department of Water Resources: Limited Printing Report LP-192, 151 p.

Larkin, R.G. and Sharp, J.M., 1992, On the relationship between river-basin geomorphology, aquifer hydraulics, and ground-water flow direction in alluvial aquifers: Geological Society of America Bulletin, v. 104, p. 1608-1620.

LBG-Guyton Associates, 2010, Appendix 3B: occurrence of significant river alluvium aquifers in the Plateau Region: Prepared for the Plateau Region Water Planning Group and Texas Water Development Board.

Lipe, J.A., Stein, L., McEachern, G.R., Begnaud, J., Helmers, S., n.d., Home fruit production- pecans: Texas Agricultural Extension Service: http://aggie-horticulture.tamu.edu/extension/homefruit/pecan/pecan.html (accessed April 2018).

Loukas, A., Vasiliades, L., Domenikiotis, C., Dalezios, N.R., 2005, Basin-wide actual evapotranspiration estimation using NOAA/AVHRR satellite data: Phyics and Chemistry of the Earth Parts A/B/C, v. 30, p. 69-79.

Maclay, R.W., and Small, T.A., 1986, Carbonate geology and hydrology of the Edwards Aquifer in the San Antonio area, Texas: Texas Water Development Board Report 296, 63 p.

McCallum, J.L., Cook, P.G., Berhane, D., Rumpf, C., and McMahon, G.A., 2012, Quantifying groundwater flows to streams using differential flow gaugings and water chemistry: Journal of Hydrology, v. 416–417, p. 118–132, doi: 10.1016/j.jhydrol.2011.11.040.

Miller, R.B., Heeren, D.M., Fox, G.A., Halihan, T., and Storm, D.E., 2016, Heterogeneity influences on stream water – groundwater interactions in a gravel- dominated floodplain: Biological Systems Engineering: Papers and Publications, 25 p., doi: 10.1080/02626667.2014.992790.

Morris, D.A. and Johnson, A.I., 1967. Summary of hydrologic and physical properties of rock and soil materials as analyzed by the Hydrologic Laboratory of the U.S. Geological Survey, U.S. Geological Survey Water-Supply Paper 1839-D, 42p.

Puente, C., 1978, Method of estimating natural recharge to the Edwards Aquifer in the San Antonio area, Texas: U.S. Geological Survey Water-Resources Investigations Report 78-10, 34 p.

Raeisi, E., 2008, Ground-water storage calculation in karst aquifers with alluvium or no-flow boundaries: Journal of Cave and Karst Studies, v. 70, p. 62–70.

Scanlon, B.R., Healy, R.W., and Cook, P.G., 2002, Choosing appropriate technique for quantifying groundwater recharge: Hydrogeology Journal, v. 10, p. 18–39, doi: 10.1007/s10040-0010176-2.

Sharp, J.M., 1988, Alluvial aquifers along major rivers, in Back, W., Rosenstein, J.S., and Seaber, P.R., eds., Hydrogeology: Boulder, Geological Society of America, The Geology of North America, v. O-2.

Sharp, J.M., Jr., Green, R.T., and Schindel, G.M., 2019, Chapter 1, Introduction, *in* Sharp, J.M., Jr., Green, R.T., and Schindel, G.M., eds., The Edwards Aquifer: The Past, Present, and Future of a Vital Water Resource: Geological Society of America Memoir 215, https://doi.org/10.1130/2019.1215(01), in press.

Singh, K., 1968, Some factors affecting baseflow: Water Resources Research, v. 4, p. 985-999.

Slade, Raymond M., Bentley, J. Taylor, Michaud, D., 2002, Results of streamflow gain-loss studies in Texas , with emphasis on gains from and losses to major and minor aquifers: US Geological Society Open-File Report 02-068, 136 p.

Slade, R., 2014, A recharge-discharge water budget and evaluation of water budgets for the Edwards Aquifer associated with Barton Springs: Texas Water Journal, vol. 5, no. 1, pg. 42-56.

Szilagyi, J.D., Rundquist, C., Gosselin, D.C., 1998, NDVI relationships to monthly evaporation: Geophysical Research Letters, v. 25, 1753-1756.

Texas Water Development Board, n.d., Groundwater database: http://www.twdb.texas.gov/groundwater/data/gwdbrpt.asp, accessed June 2017.

Todd, D. K. and Mays, L. W., 2005, Groundwater hydrology, 3rd ed.: Hoboken, NJ, John Wiley & Sons Inc., 656 p.

TNRIS, 2016, Texas statewide imagery and GIS data; Texas roadways, Texas aquifers, rivers streams and waterbodies, political boundaries, https://tnris.org/data-download/#!/statewide.

US Geological Survey, 2016, National water information system: Texas water dashboard web interface, https://txpub.usgs.gov/txwaterdashboard/index.html.

Wittenberg, H. and Sivapalan, M., 1999, Watershed groundwater balance estimation using streamflow recession analysis and baseflow separation: Journal of Hydrology, v. 219, p. 20-33.

Woodruff, C. M., Jr. and Abbott, P. L., 1979, Drainage-basin evolution and aquifer development in a karstic limestone terrane, south-central Texas, USA: Earth Surface Processes, v. 4, no. 4, p. 319-334.

Worthington, S.R.H. and Smart, C.C., 2003, Empirical determination of tracer mass for sink to spring tests in karst: Geotechnical Special Publication, doi.10.1061/40698(2003)26.